Process Design and Control Optimization: A Simultaneous Approach by Multi-Parametric Programming

Nikolaos A. Diangelakis
Centre for Process Systems Engineering, Dept. of Chemical Engineering, Imperial College London, London SW7 2AZ, U.K.

Artie McFerrin Dept. of Chemical Engineering, Texas A&M University, College Station, TX 77845

Texas A&M Energy Institute, Texas A&M University, College Station, TX 77845

Baris Burnak, Justin Katz, and Efstratios N. Pistikopoulos
Artie McFerrin Dept. of Chemical Engineering, Texas A&M University, College Station, TX 77845

Texas A&M Energy Institute, Texas A&M University, College Station, TX 77845

DOI 10.1002/aic.15825
Published online June 25, 2017 in Wiley Online Library (wileyonlinelibrary.com)

We present a framework for the application of design and control optimization via multi-parametric programming through four case studies. We develop design dependent multi-parametric model predictive controllers that are able to provide the optimal control actions as functions of the system state and the design of the process at hand, via our recently introduced PAROC framework (Pistikopoulos et al, Chem Eng Sci. *2015;136:115–138). The process and the design dependent explicit controllers undergo a mixed integer dynamic optimization (MIDO) step for the determination of the optimal design. The result of the MIDO is the optimal design of the process under optimal operation. We demonstrate the framework through case studies of a tank, a continuously stirred tank reactor, a binary distillation column and a residential cogeneration unit.* © 2017 American Institute of Chemical Engineers *AIChE J*, 63: 4827–4846, 2017
Keywords: multi-parametric programming, design and control integration, model predictive control

Introduction

The last three decades of Process Systems Engineering research and practice, have led both academia and industry to the realization that the performance of a process is affected most deterministically by its design and ability to achieve and maintain profitable operating conditions under operational uncertainty. It is also clear that the degree of interaction between those two aspects is such that one cannot be determined without the consideration of the other.[1] As a result, a number of approaches have been developed for addressing the issue of operability during the early stages of process design. Process design optimization under operational uncertainty and feasibility, flexibility, stability, controllability, and resilience metrics during process design have been extensively discussed via a series of computational methods.[2,3] This formed a prelude to the simultaneous consideration of design and control via (1) the formulation and solution of large scale optimization problems (including numerous decomposition approaches[4]), (2) flow sheet and graphical problem representations,[5] and (3) control structure selection as part of the design optimization[6] (see Table 1 for a list of publications per contribution). The control schemes employed focused mainly on PI and PID formulations while a significantly smaller portion of contributions employed model predictive control (MPC). The contributing factor to that decision was primarily the solution of the optimization problem corresponding to the control problem within a design optimization formulation.[32,49] Nevertheless, the consideration of a constrained optimization control method could contribute to overcome the shortcomings associated with PI and PID control (such as possible operational constraints violation). In the area of simultaneous design optimization with MPC notable approaches include (1) the back-off control approach,[102] (2) robust design formulations,[103] and (3) multi-parametric MPC approaches[38] (see Table 1 for a list of publications per contribution). Regarding (3), the availability of the optimal solution online via offline optimization enabled the incorporation of explicit control actions within a (mixed integer) dynamic optimization ((MI)DO) formulation thus (1) avoiding the burden of solving multiple optimization problems online, (2) transforming the control problem into a simple linear look-up function,* and

Additional Supporting Information may be found in the online version of this article.

Correspondence concerning this article should be addressed to E. N. Pistikopoulos at stratos@tamu.edu.

*The explicit solution of a model predictive control problem with a linear ($\infty-norm$) or quadratic ($2-norm$) objective function, polytopic constraints and linear state-space discrete time model dynamics is piecewise linear in the optimal actions.[104,105]

Table 1. Design and Control in the Literature

Author (year)	Contribution
Perkins & co-workers (1991),[7] Bogle & co-workers (1989, 2000),[8,9] Pistikopoulos & co-workers (1994, 1997, 2001),[10–12] Floudas & co-workers (1994, 2000, 2001),[13–15] Romagnoli & co-workers (1997),[16] Ricardez-Sandoval & co-workers (2007, 2013),[17,18] Douglas & co-workers (1988),[19–21] Skogestad & co-workers (1987, 2014),[22,23] Sorensen & co-workers (2014),[24] Stephanopoulos & co-workers (1988),[25] Ierapetritou & co-workers (2002),[26] Gani & co-workers (1995)[27]	Feasibility, flexibility, stability, controllability, and resilience considerations in steady-steady state [w/wo (MI)NLP design optimization]
Romagnoli & co-workers (1996),[28] Francisco & co-workers (2014),[29] Kravaris & co-workers (1993),[30,31]	Feasibility, flexibility, controllability, and resilience considerations in steady-steady state (MI)DO design optimization
Pistikopoulos & co-workers (2000, 2002, 2003),[32–36] Swartz & co-workers (2014),[37] Ricardez-Sandoval (2012)[3]	Simultaneous/decomposition (MI)DO process and P-PI-PID control design
Pistikopoulos & co-workers (2003, 2004),[38–41] Engell & co-workers (2004),[42] Linninger & co-workers (2007)[43]	Simultaneous/decomposition (MI)DO process and MPC design
Biegler & co-workers (2007, 2008),[4,44] Seider & co-workers (1992),[45] Ricardez-Sandoval & co-workers (2008, 2016, 2017),[46–48] Pistikopoulos & co-workers (1996),[49] Perkins & co-workers (2002, 2004, 2016),[50–52] Flores-Tlacuahuac & co-workers (2009),[53] Barton & co-workers (2010, 2011, 2015),[54–57] Mitsos & co-workers (2012),[58] Linninger & co-workers (2006)[59]	Simultaneous/decomposition/back-off via (MI)NLP
Gani & co-workers (1995, 2003, 2005, 2010),[5,27,60–62] Daoutidis & co-workers (2011),[63] Lee & co-workers (1972),[64] Chien & co-workers (2010),[65] Mitsos & co-workers (2014),[66] Luyben (2004, 2008, 2009, 2010, 2011, 2012, 2014)[67–80]	Flow sheet/graphical design and P-PI-PID control
Floudas & co-workers (1994),[13] Pistikopoulos & co-workers (1997),[81] You & co-workers (2012)[92]	Multi-objective approaches
Floudas & co-workers (2001),[15] Ierapetritou & co-workers (2002),[26] Barton & co-workers (2010, 2015),[54,57] Ricardez-Sandoval & co-workers (2013, 2015),[83,84] Pistikopoulos & co-workers (1995, 1999, 2000, 2003),[2,85–87] McRae & co-workers (2007),[88] Bogle & co-workers (2006)[89]	Design under uncertainty
Skogestad & co-workers (1987, 1989, 2014),[6,39,90] Perkins & co-workers (2002),[50] Young & co-workers (2005),[91] Stephanopoulos & co-workers (1980, 1988),[92,93] Bogle & co-workers (2010, 2016)[94,95]	Control structure selection and design
Georgiadis & co-workers (2004),[96] Francisco & co-workers (2014),[97] Ricardez-Sandoval & co-workers (2009, 2011),[98,99] Gani & co-workers (2012),[100] Mitsos & co-workers (2014)[101]	Review articles on design and control

(3) including every aspect of the MPC without any simplifications on the problem structure.

Although multi-parametric model predictive control (mpMPC) has been employed in the past in the context of simultaneous design and control optimization,[38–41] its application relied on an iterative procedure, because the control problem formulation needed to be adjusted for different design alternatives based on feasibility criteria. Here, we present a methodology, via the PAROC framework and software platform,[106] where the control problem formulation is design dependent, therefore, the explicit control actions are a function of the design variables. As a result, a single design dependent mpMPC formulation is able to control the process for bounded values of the design variables without the need of reformulation. The approach is showcased via four case studies on (1) a settling tank, (2) a continuously stirred tank reactor (CSTR), (3) a binary distillation column, and (4) a domestic cogeneration of heat and power unit.

Simultaneous Design and Control Optimization via PAROC

Given a mathematical model that describes a process based on first principles and correlations a general form of a design and control optimization problem formulation can be described as in Eq. 1.

$$\begin{aligned}
\min_{u_c,Y,De} \quad & J=\int_0^{\tau} P(x,y,u_c,Y,d,De)dt \\
\text{s.t.} \quad & \frac{d}{dt}x=f(x,u_c,Y,d,De) \\
& y_{min} \le y=g(x,u_c,Y,d,De) \le y_{max} \\
& u_c^{min} \le u_c=h(x,y,Y,d,De) \le u_c^{max} \\
& Y \in \{0,1\} \\
& [x_{min}^T,\ d_{min}^T]^T \le [x^T,\ d^T]^T \le [x_{max}^T,\ d_{max}^T]^T \\
& De_{min} \le De \le De_{max}
\end{aligned} \tag{1}$$

where, x corresponds to the system states, y to the system outputs, u_c to the optimal control actions, Y to binary variables corresponding to discrete design and operational decisions, d to uncertain, bounded system disturbances, and De to the design variables. P is the objective function that describes the operational and investment cost of the process. f and g correspond to the process dynamic and algebraic equations, respectively. h describe advanced control decisions. The system states, disturbance and design variables are assumed to be bounded. Note that the system in Eq. 1, depending on the nature of P, f, g, and h can be a non-linear, non-convex, mixed-integer dynamic problem that can rarely be tackled without simplifying assumptions that highly depend of the nature of each individual problem. Furthermore, although dynamic optimization algorithms can approximate an optimal

solution to such class problems via a variety of algorithms, the complexity arising from the simultaneous solution of the optimization based control problem and the overall design optimization still remains.[36,107] We raise the need for the latter via the development of design dependent explicit control actions via the PAROC framework and software platform[106] and their inclusion within the mixed integer dynamic optimization (MIDO) problem.

The PAROC framework and software platform

Here we present the basic principles of the PAROC framework in the context of simultaneous design and control optimization in the following steps and in Figure 1.

Step 1: "High fidelity" model—The "high fidelity" model consists of (Partial) Differential-Algebraic Equations ((P)DAE) and describes the dynamic behavior of the process. Utilizing first-principles and correlations, often non-linear in nature and high in complexity, guarantees with its robustness and quality the validity of the framework. The "high fidelity" model features the continuous and binary design variables and treats them as degrees of freedom that need to be optimally determined. The modeling takes place in PSE's gPROMS®.[107]

Step 2: Model approximation—The "high fidelity" model, although highly accurate compared to the process, is far from ideal for the application of advanced optimization techniques. Its dynamic nature and high complexity require an approximation step in order for approaches such as multi-parametric programming to be considered. With (1) model accuracy preservation and (2) complexity reduction in mind the approximation step takes place via model reduction techniques[108] and/or the statistical methods (System Identification toolbox, MATLAB®). The key for this step is the preservation of the design variables in the approximation step, i.e., the derivation of linear state-space models that include the design variables in the model expressions, symbolically described in Eqs. 2 and 3.

"High fidelity" model

$$\begin{aligned} &\frac{d}{dt}x(t)=f(x(t),u_c(t),Y(t),d(t),De)\\ &y=g(x(t),u_c(t),Y(t),d(t),De) \end{aligned} \tag{2}$$

Approximate model

$$\begin{aligned} &x_{T+1}=A\cdot x_T+B\cdot u_{c,T}+C\cdot\begin{bmatrix} d_T\\ \\ De\end{bmatrix}\\ &y_T=D\cdot x_T+E\cdot u_{c,T}+e \end{aligned} \tag{3}$$

Note the following:

- The states $x\in\mathbb{R}^{q_1}$ in Eqs. 2 and 3 may have different physical meanings due to the approximation step.[106] The optimization variables $u_c\in\mathbb{R}^n$, outputs $y\in\mathbb{R}^{q_2}$, disturbances $d\in\mathbb{R}^{q_3}$ and design variables $De\in\mathbb{R}^{q_4}$ have the same physical meaning in both instances.
- The approximate model is presented here in a discrete time formulation. Continuous time formulations can be derived equivalently.
- The binary variables $Y\in\{0,1\}^r$ present in the "high fidelity" model may result in multiple approximate state-space models or piecewise affine formulations (omitted here).
- The design variables De are not time dependent since the design of the process cannot change during operation.
- The design of the process is treated as a measured additive uncertainty within the approximate model via the term De. Multiplicative uncertainty can be incorporated without any changes in the framework. This can be achieved via the consideration of robust mpMPC as described in Refs. 109–111. In such case, the use of state-estimators is also necessary.[112–114]
- The vector d_T in Eq. 3 introduces disturbances as uncertain bounded parameters to the approximate state-space models. The values of d_T are assumed to remain constant within the discretization time step (piecewise constant) and measurable at time T but not prior to that. Within the multi-parametric framework, the vector d_T is treated as a vector of unknown but bounded parameters, similarly to the states at $T=0$.[104,115]
- The term e corresponds to a mismatch between the real, measured system output and the approximate state-space model output at the first time step and assumed fixed throughout the horizon of the optimization formulation.

The system described in 3 can be used for advanced optimization based control formulations such as mpMPC resulting into a quadratic problem with linear constraints.[†]

Step 3: Multi-parametric programming—The design of the controllers is based on the validated procedure described in Refs. 104, 106, 116. Equation 4 shows the form of a typical mpMPC controller.

$$\begin{aligned} \min_u\quad & J=x_N^TPx_N+\sum_{k=1}^{N-1}\left(x_k^TQ_kx_k+\left(y_k-y_k^R\right)^TQR_k\left(y_k-y_k^R\right)\right)+\\ &+\sum_{k=0}^{M-1}\left(\left(u_{c,k}-u_{c,k}^R\right)^TR_k\left(u_{c,k}-u_{c,k}^R\right)+\Delta u_{c,k}^TR1_k\Delta u_{c,k}\right)\\ \text{s.t.}\quad & x_{k+1}=A\,x_k+B\,u_{c,k}+C\,d_k\\ & y_k=D\,x_k+E\,u_{c,k}+e\\ & u_{min}\le u_{c,k}\le u_{max}\\ & \Delta u_{min}\le\Delta u_{c,k}\le\Delta u_{max}\\ & x_{min}\le x_k\le x_{max}\\ & y_{min}\le y_k\le y_{max} \end{aligned} \tag{4}$$

where x_k are the state variables, $u_{c,k}$ and $u_{c,k}^R$ are the control variables and their respective set points, Δu_k denotes the difference between two consecutive control actions, y_k and y_k^R are the outputs and their respective set points, d_k concatenation of the system disturbances and design variables, Q_k, R_k, $R1_k$, and QR_k are their corresponding weights in the quadratic objective function, P is the stabilizing term derived from the Riccatti Equation for discrete systems, N and M are the output horizon and control horizon, respectively, k is the time step, A, B, C, D, E are the matrices of the discrete linear state space model and e denotes the mismatch between the actual system output and the predicted output at initial time. Here, the d_k vector includes all the variables that cannot be manipulated via the MPC problem, hence it includes the design variables as well. In the context of multi-parametric programming the latter are treated as parameters.

[†]In the case of multiplicative uncertainty the framework presented in Ref. 110 can be utilized to derive the optimal control strategies

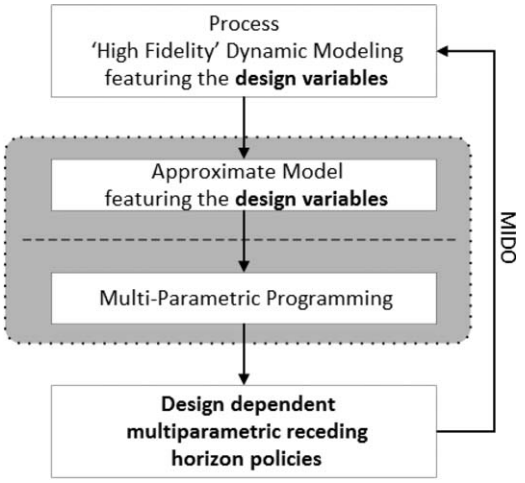

Figure 1. The PAROC framework approach for simultaneous design and control. Actions within the gray area happen once and offline.

The resulting multi-parametric program (Eq. 5) is solved via the POP® toolbox in MATLAB®, thus acquiring a map of optimal control actions.[117]

$$\begin{aligned} \min_{u_c} \quad & J=\frac{1}{2}u_{c,T}^T H u_{c,T}+u_{c,T}^T F^T \theta_T \\ \text{s.t.} \quad & W u_{c,T} \le S+Z\theta_T \\ & u_{c,T} \in U=\{u_{c,T} \in \mathbb{R}^n | u_{min} \le u_{c,T} \le u_{max}, \forall n\} \\ & \theta_T \in \Theta=\{\theta_T \in \mathbb{R}^q | \theta_{min} \le \theta_T \le \theta_{max}, \forall q\} \end{aligned} \tag{5}$$

Due to the form of the approximate model and the MPC formulation, the resulting explicit control actions are an affine function of the design variables (Eq. 6).

$$\begin{aligned} & u_{c,T}=K_i\theta_T+r_i, \ \ \forall \theta_T \in CR_i \\ & \theta_T=[x_T; u_{c,T-1}; d_T; De; y_T; y_T^{SP}] \end{aligned} \tag{6}$$

where x_T, d_T, y_T, y_T^{SP} are the states, measured disturbances, outputs and output set points, respectively, $u_{c,T-1}$ are the optimal control action at the previous time step and De are the design variables (fixed throughout the optimization horizon of the control problem). It is clear from Eq. 6 that the optimal action is a function of the operation of the system (via x_T and y_T), the presence of disturbances, the operating set points and, most importantly for the simultaneous design and control framework, the design variables.

More specifically, let θ_T^* denote a value realization of the parametric vector and $u_{c,T}^*$ be the corresponding optimal actions. The i^{th} Active Constraint set of cardinality j is denoted by $\hat{W}$, $\hat{S}$, and $\hat{Z}$ the inactive set by $\check{W}$, $\check{S}$, and $\check{Z}$ and LICQ holds. λ_i^* correspond to the j Lagrange multipliers of the Active Set. The Karush-Kuhn-Tucker conditions for the strictly convex problem 5 are presented in Eq. 7.

$$\begin{aligned} & \hat{W}u_{c,T}^*=\hat{S}+\hat{Z}\theta_T^* \\ & Hu_{c,T}^*+F^T\theta_T^*+\hat{W}^T\lambda_i^*=0 \end{aligned} \tag{7}$$

Solving the above for $u_{c,T}^*$ and λ_i^* we obtain the parametric expressions:

$$\begin{aligned} & \lambda_i^*(\theta_T^*)=(\hat{W}H^{-1}\hat{W}^T)^{-1}(\hat{W}H^{-1}F^T+\hat{Z})\theta_T^*-(\hat{W}H^{-1}\hat{W}^T)^{-1}\hat{S} \\ & u_{c,T}^*(\theta_T^*)=\underbrace{\left[H^{-1}\hat{W}^T(\hat{W}H^{-1}\hat{W}^T)^{-1}(\hat{W}H^{-1}F^T+\hat{Z})-H^{-1}F^T\right]}_{K_i} \\ & \theta_T^*\underbrace{-H^{-1}\hat{W}^T(\hat{W}H^{-1}\hat{W}^T)^{-1}\hat{S}}_{r_i} \end{aligned} \tag{8}$$

Hence, the values K_i and r_i are analytically derived as the coefficients of Eq. 8 for the i^{th} Active Set. The composite polyhedron CR_i is calculated by postulating the j Lagrange multipliers to be larger than zero and the unconstrained set to remain strictly unconstrained (Eq. 9). The coefficients derived above are optimal for realizations of θ_T within the composite polyhedron CR_i hence the generalized version presented in Eq. 6.

$$CR_i=\begin{cases} \check{W}u_{c,T}^*(\theta_T)-\check{S}-\check{Z}\theta_T < 0 \\ (\hat{W}H^{-1}\hat{W}^T)^{-1}(\hat{W}H^{-1}F^T+\hat{Z})\theta_T-(\hat{W}H^{-1}\hat{W}^T)^{-1}\hat{S} > 0 \end{cases} \tag{9}$$

For a complete review of multi-parametric programming, properties of the solution and available solution techniques and algorithms the reader is referred to Ref. 118.

From the derivation of the explicit/multi-parametric solution and the critical regions the following can be stated in context with the framework presented here:

- **Exact MPC solution**: the solution of the multi-parametric quadratic programming problem presented in Eq. 5 is solved once and offline and the exact solution is obtained for any feasible value of the uncertain parameters θ_T.
- **Optimal partitioning of the parametric space**: the feasible parametric space is partitioned optimally, a fact that follows the generalization of the KKT conditions in the parametric space of a convex (with respect to the optimization variables $u_{c,T}$) quadratic problem with regards to its parameters.
- **Ease of online application**: the nature of the dependency of the critical regions CR_i and optimal actions $u_{c,T}$ with respect to the parameters reduces the online application of the MPC to a simple look-up table algorithm (commonly referred to as the point location problem) and function evaluations, all affine. Therefore the online application of the mpMPC is similar in complexity with a simple PI controller.
- **Online application computational time**: a significant, direct result of the above is the reduction of the online computational time in the range of a few milliseconds per action which results into a very efficient simultaneous application of MPC within a simulation or optimization context.‡
- **Space requirements of the solution**: the partitioning of the space can result into the creation of a large number of critical regions that may require significant computational space to be saved. Although typically the space requirements here were not an issue (less than 1 MB per solution) it is likely that solutions that require several MBs of computational space can be obtained. The space requirements can be significantly reduced by manipulating the floating point precision of the solution (i.e., acquiring a solution with as little

‡The statistics for such a claim result from the online application of the controllers within gPROMS® via C++ programming, as described in Step 4.

Table 2. An Indicative List of (MI)DO Algorithms in Literature

Author (year)	Contribution
Pistikopoulos & co-workers (2003)[120]	Algo. 1: GBD based approach. The master problem is constructed without the solution of an intermediate adjoint problem at the expense of including additional equations and search variables Algo. 2: Master problems are computationally more expensive due to addition of linearizations about the optimal solution of the primal problem. Additional constraints render the master problem tighter, hence fewer iterations suffice for a local solution
Barton & co-workers (2006, 2009)[121,122]	Algo. 1: Outer approximation based approach for global optimization. Primal problem is not solved to global optimality at every iteration, which alleviates the computational burden Algo. 2: Formulates a bilevel dynamic optimization problem, which can be naturally extended to a mixed-integer dynamic optimization formulation. A branch and bound algorithm is utilized to solve the problem to global optimality
Biegler & co-workers (2007)[123]	Full discretization by finite elements, and solving a large scale nonconvex MINLP. Generalized disjunctive programming are used to solve the MINLP
Marquardt & co-workers (2008)[124]	MIDO problem is reformulated as a mixed-logic dynamic optimization problem, and solved by control vector parameterization and direct multiple shooting
You & co-workers (2013, 2014, 2015)[125–130]	Algo. 1: The inner level dynamic optimization problem is replaced with a set of surrogate models, which are updated adaptively with every iteration Algo. 2: MIDO is reformulated as a large scale MINLP problem. MILP master problem is subjected to a bilevel decomposition algorithm based on the inherently different time scales of the original problem Algo. 3: GBD based approach. Decomposed primal problem is a set of separable dynamic optimization problems, and the master problem is a mixed-integer nonlinear fractional problem, which is solved to global optimality by a fractional programming algorithm

as a few decimals instead of the 16 decimals working precision of most software tools without affecting the precision of the applied optimal action) or with recent techniques such as the ones described in Ref. 119.

Step 4: Closed-loop validation—The framework is validated through closing the loop against the original model of Step 1. This can happen either via the interoperability between software tools such as gPROMS® and MATLAB® via gO:MATLAB or via the straight implementation of the controllers in the gPROMS® simulation via the use of C++ programming and the creation of Dynamic Link Libraries. Note that the validation step is necessary in order to test the behavior of the control scheme for a variety of different control and process designs. Given that the design dependent control scheme can satisfactorily handle the operation of the system for different designs (efficient set point tracking, constraint violation, stable operation are some of the criteria), the simultaneous design and control optimization can take place. Note that in this work the approximate state-space models on which the control schemes are derived treat the design variables as measured added disturbances, a relationship that is not always the same in the "high-fidelity" model. The purpose of this step is also to verify whether such an approximation results in acceptable control behavior for different designs.

Step 5: Dynamic optimization—Through the creation of Dynamic Link Libraries the design dependent control scheme is introduced into gPROMS®. Problem 1 is therefore reformulated as in Eq. 10.

$$\begin{aligned}
\min_{u_{c,T},Y,De} \quad & J=\int_0^{\tau} P(x,y,u_c,Y,d,De)dt \\
\text{s.t.} \quad & \frac{d}{dt}x=f(x,u_c,Y,d,De) \\
& y_{min} \le y=g(x,u_c,Y,d,De) \le y_{max} \\
& u_{c,T}=K_i(\theta_T)+r_i, \ \ \forall \theta_T \in CR_i \\
& \theta_T=[x_T; u_{c,T-1}; d_T; De; y_T; y_T^{SP}] \\
& Y \in \{0,1\} \\
& [x_{min}^T, \ d_{min}^T]^T \le [x^T, \ d^T]^T \le [x_{max}^T, \ d_{max}^T]^T \\
& De_{min} \le De \le De_{max}
\end{aligned} \tag{10}$$

Problem 10 is a MIDO program which is handled via a control vector parameterization (CVP) algorithm in gPROMS®. The term T denotes the control time step interval and τ the horizon of the MIDO problem. The time-varying optimization variables are piecewise-constant functions of time over a number of intervals which are specified by the user according to the needs of each problem. Note that the duration of the intervals in each step are in this case determined by the user to be equal in duration with the control time step for synchronization purposes.[§] The single vector shooting dynamic optimization can be decomposed as follows[¶]:

- The values of the optimization variables are determined for each interval.
- The dynamic model is simulated over the entire time horizon.
- The value of (1) the objective function and its partial derivatives with respect to the optimization variables and (2) the constraints are determined.
- Convergence is checked and if needed the steps are repeated.

According to the Optimization Guide of PSE's gPROMS® the CVP algorithm for (MI)DO relies on the values of the partial derivatives of the problem's objective function with respect to the optimization variables to determine its next iteration step. In the case of the design optimization variables, the partial derivatives are needed with respect to the rest of the "high-fidelity" model variables (x and y) as well as the control variables ($u_{c,T}$). Although the derivatives of the former are calculated "on the fly" via the optimization algorithm, the calculation of the derivatives of the latter can become an issue

[§]In the general case this is an extra degree of freedom for the dynamic optimizer.
[¶]For more information the user is referred to the optimization guide of PSE's gPROMS®.

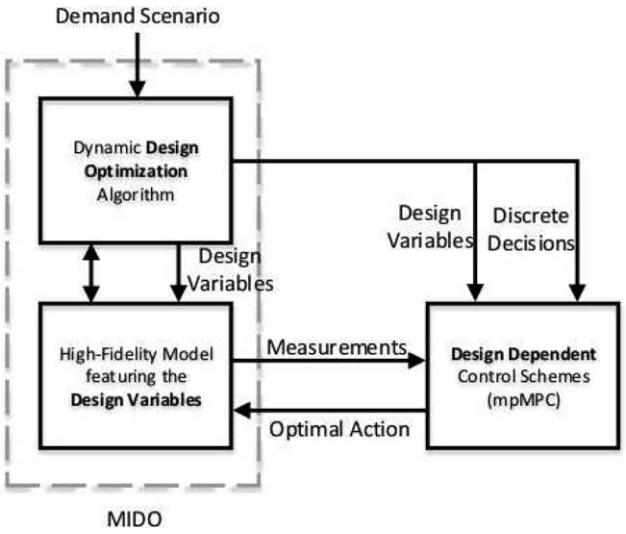

Figure 2. Schematic representation of the simultaneous design MIDO with embedded mpMPC. The area within the dashed line represents the MIDO problem.

when an external piece of software introduces the $u_{c,T}$ values to the problem. This burden is alleviated with the use of mpMPC as the partial derivatives of the control actions with respect to the design variables (optimization variables in the (MI)DO context) are available *a priori* via K_i in Problem 10 as exact expressions, not numerical approximations, thus utilizing in full the concept of "map of solutions" introduced in Ref. 109. Also note that the dynamic model simulation in gPROMS® happens based on non-uniform discretization steps posing a technical, time synchronization challenge to the overall simultaneous approach. In order to overcome this, an error function is defined for every control action which absorbs the evaluation of the controller at the non-uniform time steps of the simulation and only utilize the evaluation at the control time intervals. This happens via imposing interior point constraints of the form $err(t)=u_{c,T}-u(t)=0$. The latter is zero only at every interior point of the MIDO. The variable $u(t)$ therefore remains piecewise constant, between interior points, and equal to the value of $u_{c,T}$ at the interior point, although from a software point of view the variable $u_{c,T}$ is free to be evaluated multiple times throughout a single MIDO time step. The evaluation of $u_{c,T}$ within the MIDO time step is therefore rejected. Also note that within the MIDO problem, the optimal control action $u_{c,T}$ is regarded as an optimization variable although it is calculated via the mpMPC formulation of Step 3. The two reasons that this is happening is (1) the fact that the action is implicitly optimized via the optimal choice of the design variables *De* and the dependence of $u_{c,T}$ to those variables and (2) the fact that within the MIDO problem formulation this is necessary in order to achieve the synchronization of the fixed time-step control with the MIDO problem.

Based on the nature of the design dynamic optimization model and especially the existence of binary variables, suitable optimization solvers are employed for the task of optimizing the model at every interval. More specifically, for the general case of MIDO an Outer approximation based method is employed where the problem is initially reformulated to a completely relaxed NLP. A linearized version of the model excluding any binary variable combinations from previous iterations is subsequently solved (master problem). Based on the integer solution of the master problem, the primal problem is formulated and solved. Both the primal and the fully relaxed problem are solved via a sequential quadratic programming algorithm. Note that in this work we use a commercially available software tool for the solution of the design (MI)DO problem. Based on the aforementioned characteristics of the solver the solution is guaranteed to be locally optimal, even for the DO case. For a list of available MIDO algorithms see Table 2. The overall simultaneous design and control optimization is schematically presented in Figure 2. The dynamic optimization algorithm utilizes information from the process and the optimal control actions derived multi-parametrically to determine the optimal design. The values for the optimal design are used to calculate the numerical values of the control actions and progress the simulation step.

The following sections present the application of the simultaneous design and control framework via a tank, a CSTR, a binary distillation column and a domestic cogeneration unit examples.

The Tank Example

This case study focuses on the design of a simple tank. A sinusoidal inlet flow signal is introduced to a tank the outlet of which is manipulated via a mpMPC. The purpose of the controller is to maintain a certain liquid volume within the tank regardless of the inlet. The sinusoidal form of the inlet is handled as a bounded parametric uncertainty via the control problem, its nominal value and deviation is dynamically optimized to determine the maximum deviation from the nominal value for which the controller can maintain a liquid volume setpoint. Given a correlation between the tank set point, the nominal flow and its deviation the set point is dynamically calculated and therefore so is, implicitly, the volume of the tank. The set point is determined as a function of the nominal value and maximum deviation of the sinusoidal inlet flow rate. The tank volume is therefore inferred by that. Note that in order to maintain the set point in time and reduce the size of the dynamic optimization the dynamic optimization problem is limited to one period of the inlet sinusoidal wave. Constraints within the dynamic optimization ensure that the initial point of the optimization is the same as the final point, therefore achieving a cyclic operation that allows for the extrapolation of the operation to larger horizons.

"High fidelity" dynamic modeling

The model of the tank is presented in Eq. 11

Table 3. Weight Tuning for the mpMPC of the Tank

MPC design parameters	Value
N	10
M	1
$QR_k, \forall k \in \{1,\ldots,\mathrm{N}\}$	10
$R_k, \forall k \in \{1,\ldots,\mathrm{M}\}$	10^{-7}
x_{min}	-10^3
x_{max}	10^3
u_{min}	0
u_{max}	1
y_{min}	0
y_{max}	10
d_{min}	0
d_{max}	5

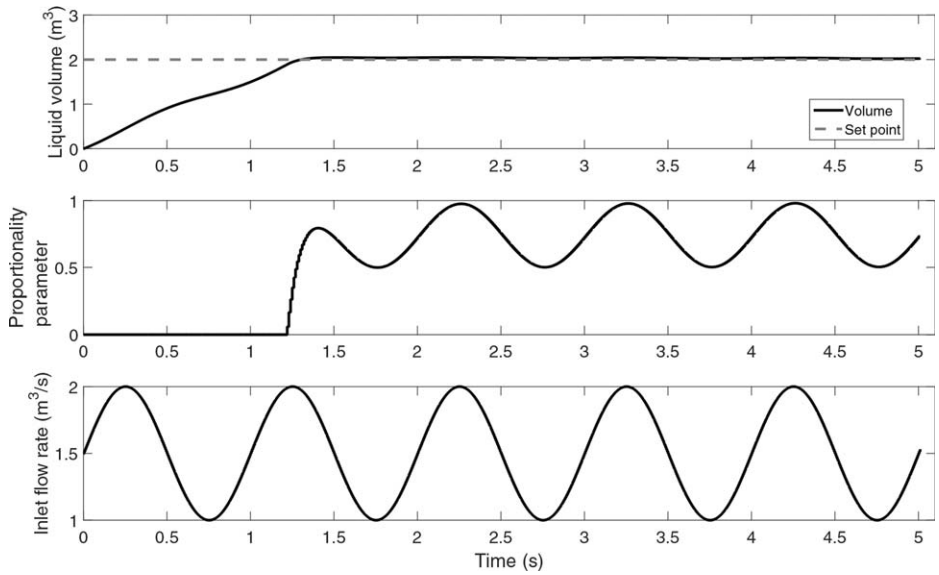

Figure 3. Closed loop validation of the controller against the high fidelity model.

$$\begin{aligned} \frac{dV}{dt} &= F_{in} - F_{out} \\ F_{out} &= a \cdot V \\ F_{in} &= F_{nom} + F_{dev} \cdot \sin\left(t/freq\right) \\ freq &= \frac{1}{2 \cdot \pi} \end{aligned} \tag{11}$$

where V is the volume of the liquid within the tank, F_{in} and F_{out} the inlet and outlet flow rate, a is a proportionality parameter and the control variable, F_{nom} and F_{dev} are the nominal inlet flow rate and its deviation and $freq$ is the sinusoidal signal frequency. Note that V is the state of the system and is bilinear with the control variable a which makes the linearization of the system necessary for multi-parametric programming. Alternatively, a robust reformulation of the system in discrete time would alleviate the need of approximation resulting in the consideration of the exact model in the multi-parametric programming formulation. In this context, F_{in} being treated as bounded parametric uncertainty, doesn't interfere with the linearity of the state-space formulation.

Model approximation

The approximation of the tank model in Eq. 11 takes place in the System Identification Toolbox in MATLAB® and results into the linear state-space in Eq. 12.

$$\begin{aligned} x_{T+1} &= 0.9980 \cdot x_T - 0.2536 \cdot u_{c,T} + 0.1003 \cdot d_T \\ y_T &= 109.9320 \cdot x_T - 2.0378 \cdot u_{c,T} \\ T_s &= 0.01s \end{aligned} \tag{12}$$

where x_T are the identified states, $u_{c,T}$ is the proportionality parameter, d_T is the flow at the inlet of the tank, and y is the liquid volume in the tank.

The step and impulse responses of the system are presented in Figures B1a, B1b, respectively.

Design of the multi-parametric model predictive controller

The multi-parametric model predictive controller problem is formulated and solved using POP where the optimal control action is generated as a map of solutions and as a function of the problem parameters.[104,117] The problem formulation is based on Eq. 4 and the tuning of the controller is presented in Table 3.

The design variable corresponding to the volume of the tank is introduced as a parameter at the upper bound of the output of the system. Furthermore, the bounds for the disturbance of the system d_{min} and d_{max} have been chosen such that $d_{min} = F_{nom,min} - F_{dev,\max}$ and $d_{max} = F_{nom,max} + F_{dev,max}$. The purpose of the controller is to maintain the volume of the liquid within the tank at a certain set point with a maximum deviation of less than 5%, effectively rejecting the disturbance introduced at the inlet of the tank.

Closed-loop validation

The validation step is presented in Figure 3 where the controller is tested against the original high fidelity model. The closed loop validation of the controller happens for the following process characteristics:

- Nominal inlet flow rate: $1.5\,\mathrm{m}^3/\mathrm{s}$
- Inlet flow rate deviation: $0.5\,\mathrm{m}^3/\mathrm{s}$
- Volume set point: $2\,\mathrm{m}^3$

Note that in the case of the tank the set point for the volume V^{SP} is dynamically correlated with the maximum value of the inlet flow rate (i.e., if $F_{in} = F_{nom} + F_{dev} \cdot \sin\left(t/freq\right)[\mathrm{m}^3/\mathrm{s}]$ then $V^{SP} = (F_{in} + F_{out}) \times 1s[\mathrm{m}^3]$).

Dynamic optimization

The dynamic optimization in Problem 10 is formulated in order to find the maximum value of F_{dev} for which the system can track a volume set point. The F_{nom} value is an optimization variable for the dynamic optimization problem. Furthermore, the optimization formulation considers the initial point of the state variables as optimization variables. This is to ensure that the starting point and the end point of the optimization problem will coincide, resulting in a cyclic operation. The full dynamic optimization problem is presented in Eq. 13. The problem is run for 1 s (1 cycle for the disturbance sinusoidal signal), i.e., for 100 intervals.

$$
\begin{aligned}
\max_{V_{tank},F_{dev},F_{nom},V(t=0),x(t=0)} \quad & J=\int_0^1 F_{dev}dt \\
\text{s.t.} \quad & \frac{dV(t)}{dt}=F_{in}(t)-F_{out}(t) \\
& F_{out}(t)=a_T\cdot V(t) \\
& F_{in}(t)=F_{nom}+F_{dev}\cdot \sin\left(t/freq\right) \\
& freq=\frac{1}{2\cdot\pi} \\
& \text{mpMPC}(t)=K_i\cdot[x(t),F_{in}(t),V(t),V^{SP}]^T+r_i, \\
& \forall[x(t),F_{in}(t),V(t),V^{SP}]^T\in CR_i \\
& V^{SP}=F_{nom}+F_{dev}\le V_{tank} \\
& err_{\text{mpMPC}}=\int_0^1\frac{||V(t)-V^{SP}||}{V^{SP}}dt \\
& \text{End point constraints} \\
& x(t=0)=x(t=1)\ ,\ \text{states of the state}-\text{space model} \\
& V(t=0)=V(t=1),\text{statesofthe highfidelity/model} \\
& err_{\text{mpMPC}}\le 1\% \\
& \text{Interior point constraint } \forall T\in\{1,\ldots,100\} \\
& \text{mpMPC}(t=T)-a_T=0
\end{aligned}
\tag{13}
$$

End point constraints in the optimization problem are introduced to allow for a set point deviation of less than 1% per cycle and to ensure cyclic operation. The purpose of the interior point constraint at every interval is to use the controller evaluation only at the beginning of every intervals as a piecewise constant value. The dynamic optimization yields a nominal inlet flow rate of $2.485\,\text{m}^3/\text{s}$ with an equal deviation. The initial volume for cyclic operation has been identified as $V=4.99\,\text{m}^3$. Furthermore, due to the maximum controller error consideration the volume of the tank is $5.0694\,\text{m}^3$. The error of the mpMPC at the end of a single cycle is 0.9%.

The CSTR Example

A fixed volume CSTR is used here as a case study for simultaneous design and control optimization. The goal is to optimize the volume of the tank reactor assuming perfect control at the outlet of the reactor, (i.e., the total outlet flow rate at the outlet of the reactor is determined by the inlet and no other phenomena are assumed to affect it.). The concentration of the reactants and mass flow rate at the inlet of the reactor are treated as known and unknown disturbances, respectively. A sinusoidal behavior of flow and concentration is assumed. The sinusoidal form of the inlet is handled as a bounded parametric uncertainty via the control problem, its nominal value and deviation is dynamically optimized at the MIDO step to determine the maximum deviation from the nominal value for which the controller can maintain a minimal reactant concentration at the outlet of the CSTR. On the contrary to the previous example, here we take into account the possibility of having a settling tank prior to the CSTR that will stabilize the inlet flow. Its cost of equipment and operation is taken into account in the overall cost minimization of the CSTR, which is the objective of the design optimization problem. A multi-

Table 4. Weight Tuning for the mpMPC of the CSTR

MPC design parameters	Value
N	3
M	3
$QR_k,\forall k\in\{1,\ldots,\text{N}\}$	5×10^5
$R_k,\forall k\in\{1,\ldots,\text{M}\}$	1
x_{min}	$[0\quad 100]^T$
x_{max}	$[20\quad 450]^T$
u_{min}	200
u_{max}	500
y_{min}	$[0\quad 100]^T$
y_{max}	$[20\quad 450]^T$
d_{min}	$[0\quad 500]^T$
d_{max}	$[20\quad 1000]^T$

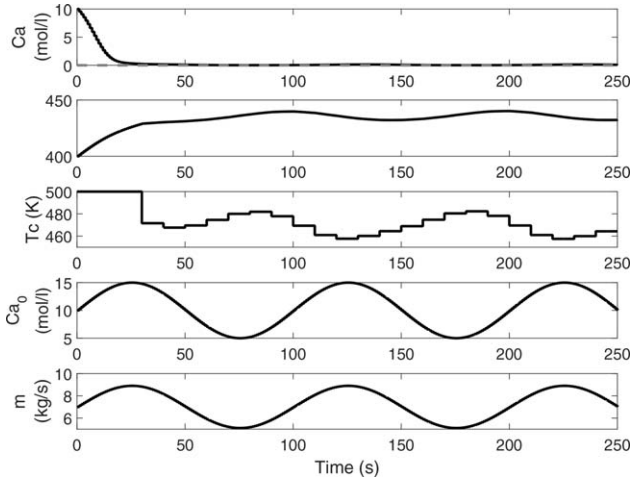

Figure 4. Closed loop validation of the controller against the high fidelity model.

(a) Tank usage for a fixed initial $Ca_{0,nom}=10\,\text{mol/L}$(optimal). (b) Tank usage for a fixed initial $Ca_{0,nom}=8\,\text{mol/L}$.

Table 5. Characteristic Equations for a Binary Distillation Column

Description	Equation
Component mass balance	$\frac{dM_{i,k}}{dt}=L_{k+1}x_{i,k+1}+V_{k-1}y_{i,k-1}+F_k z_{i,f}+R_k x_{i,D}-L_k x_{i,k}-V_k y_{i,k},\ \forall k\in\{2\ldots Ntrays-1\}$
Total mass balance	$\frac{dM_k}{dt}=L_{k+1}+V_{k-1}+F_k+R_k-L_k-V_k,\ \forall k\in\{2\ldots Ntrays-1\}$
Vapor molar flow rate	$V_k=V_{k-1}=V_B,\ \forall k\in\{2\ldots Ntrays-1\}$
Hold-up	$Vol_k=\frac{M_k}{\rho_{Lmix,k}}$
Liquid level	$Level_k=\frac{L_k^{2/3}}{1.84\rho_{Lmix,k}L_{weir}}+H_{weir}$
Tray area	$A_{tray}=\frac{0.8\pi D_c^2}{4}$
Weir length	$L_{weir}=0.77D_c$
Reboiler vapor liquid equilibrium	$1=\frac{P^0_{benz,B}x_{i,B}+P^0_{tol,B}(1-x_{i,B})}{P}$
Condenser vapor liquid equilibrium	$1=P(\frac{x_{i,D}}{P^0_{benz,D}}+\frac{1-x_{i,D}}{P^0_{tol,D}})$
Relative volatility	$\alpha=\sqrt{\frac{P^0_{benz,D}P^0_{benz,B}}{P^0_{tol,D}}P^0_{tol,B}}$
	$y_{i,k}=\frac{\alpha x_{i,k}}{1+x_{i,k}(\alpha-1)}$
Reboiler and reflux drum molar balance	$\frac{dM_{i,B}}{dt}=L_1x_{i,1}-Bx_{i,B}-V_By_{i,B}$
	$M_B=\frac{M_{i,B}}{x_{i,B}}$
	$\frac{dM_{i,D}}{dt}=V_{Ntrays}(y_{i,Ntrays}-x_{i,D})$
	$M_D=\frac{M_{i,D}}{x_{i,D}}$
Reboiler and reflux drum energy balance	$0=L_1-B-V_B$
	$0=V_D-\Sigma R_k-D$

Component i is benzene, tray number is $k\in\{1\ldots Ntrays\}$ unless stated otherwise.

parametric controller is introduced to manipulate the temperature of the heating jacket in order to minimize the concentration of the reactants at the outlet.

"High fidelity" dynamic modeling

The model of the CSTR is presented in Eq. 14

$$\frac{dCa}{dt}=\frac{m}{\rho\cdot V}\cdot(Ca_0-Ca)-k_0\cdot Ca\cdot e^{\frac{-E_a}{R\cdot T}}$$

$$\frac{dT}{dt}=\frac{m\cdot C_p\cdot(T_0-T)+V\cdot\Delta H_{rxn}\cdot Ca\cdot k_0\cdot e^{\frac{-E_a}{R\cdot T}}+UA\cdot(T_c-T)}{V\cdot\rho\cdot C_p}$$

$$Ca_0=Ca_{0,nom}+Ca_{0,dev}\cdot\sin(t/freq)$$

$$m=m_{nom}+m_{dev}\cdot sw_{y_b}$$

$$\frac{dsw_{y_b}}{dt}=y_b\cdot(1/freq)\cdot\cos(t/freq)$$

$$freq=100/(2\cdot\pi) \tag{14}$$

where Ca and Ca_0 is the concentration of the reactants in the reactor and at the inlet, respectively, m is the mass flow rate at the inlet and outlet of the reactor, V is the volume of the reactor, k_0 is the rate constant of the reaction, E_a is the activation energy, R is the ideal gas constant, T is the temperature in the reactor and at the reactor outlet, C_p is the overall heat capacity, T_0 is the temperature of the inlet flow stream, ΔH_{rxn} is the rate of reaction, UA is the overall heat transfer coefficient, and T_c the temperature in the heating jacket of the reactor. C_a and T are the states of the system, T_c is the control variable, and V is the design variable. The last four equations of the model represent the sinusoidal form of the disturbances. The binary variable y_b denotes the existence and operation or not of a settling tank prior to the CSTR. Notice that the binary variable appears in the differential form of the sinusoidal wave in order to affect the rate of change of the concentration and mass flow rate rather than the value itself.

Model approximation

The approximation of the tank model in Eq. 14 takes place in the System Identification Toolbox in MATLAB® and results into the linear state-space in Eq. 15.

$$x_{T+1}=\begin{bmatrix}0.9627 & 0.006032\\ 0.7177 & 0.8839\end{bmatrix}\cdot x_T+\begin{bmatrix}-0.005116\\ 0.09858\end{bmatrix}\cdot u_{c,T}+\begin{bmatrix}-0.02026 & -9.429\cdot10^{-5}\\ 0.384 & 0.001842\end{bmatrix}\cdot\begin{bmatrix}d_T\\ De\end{bmatrix}$$

$$y_T=\begin{bmatrix}1 & 0\\ 0 & 1\end{bmatrix}\cdot x_T \tag{15}$$

$$T_s=10s$$

where x_T are the identified states, $u_{c,T}$ is the temperature of the jacket, d_T is the concentration of the reactants at the inlet of the CSTR, De is the volume of the CSTR, and y is the concentration of the reactants at the outlet of the reactor and the temperature of the outlet stream.

The step and impulse responses of the system are presented in Figures B2a, B2b, respectively.

Design of the multi-parametric model predictive controller

The multi-parametric model predictive controller problem is formulated based on Eq. 4 and solved with POP.[117] The objective of the mpMPC is to minimize the concentration of the reactants at the outlet of the reactor. The tuning of the controller is presented in Table 4.

The purpose of the controller is to minimize the concentration of the reactant at the outlet of the CSTR and effectively reject the disturbances at the concentration introduced at the inlet.

Closed-loop validation

The validation step is presented in Figure 4 where the controller is tested against the original high fidelity model. Here it is assumed that no settling tank exists prior to the CSTR (i.e., $y_b=1$). The closed loop validation of the controller happens for the following process characteristics:

- CSTR Volume: $750\,m^3$
- $Ca_{0,nom}$: $3\,mol/L$
- $Ca_{0,dev}$: $1\,mol/L$
- m_{nom}: $2\,m^3/s$
- m_{dev}: $0.5\,m^3/s$

Dynamic optimization

The objective of the dynamic optimization is to determine (1) the optimal volume of the CSTR, (2) the necessity for a settling tank prior to the CSTR and its settling time (3) the nominal and deviation values for the concentration of reactants and flow rate at the inlet of the reactor. This is done by minimizing a total cost function as shown in Eq. 16. At the starting point of the optimization, we assume that both the Ca_0 and m start at their nominal value.

$$
\begin{aligned}
\max_{V,m_{dev},m_{nom},Ca_{dev},Ca_{nom},y_b} \quad & J=Cost_{Total} \\
\text{s.t.} \quad & \frac{dCa(t)}{dt}=\frac{m(t)}{\rho\cdot V}\cdot(Ca_0(t)-Ca(t))-k_0\cdot Ca(t)\cdot e^{\frac{-E_a}{R\cdot T(t)}} \\
& \frac{dT(t)}{dt}=\frac{m(t)\cdot C_p\cdot(T_0-T(t))+V\cdot\Delta H_{rxn}\cdot Ca(t)\cdot k_0\cdot e^{\frac{-E_a}{R\cdot T(t)}}+UA\cdot(T_{c,T}-T(t))}{V\cdot\rho\cdot C_p} \\
& Ca_0=Ca_{0,nom}+Ca_{0,dev}\cdot\sin(t/freq) \\
& m=m_{nom}+m_{dev}\cdot sw_{y_b} \\
& \frac{dsw_{y_b}}{dt}=y_b\cdot(1/freq)\cdot\cos(t/freq) \\
& freq=100/(2\cdot\pi) \\
& \text{mpMPC}(t)=K_i\cdot[x(t),Ca_0(t),V(t),Ca(t),T(t),Ca^{SP}]^T+r_i, \\
& \forall[x(t),Ca_0(t),V(t),Ca(t),T(t),Ca^{SP}]^T\in CR_i \\
& Ca^{SP}=0 \\
& \text{Objective function} \\
& Cost_{Total}=Cost_{Equipment}+Cost_{Operational} \\
& Cost_{Equipment}=10\cdot((V-750)/\pi)+1000+400\cdot y_{b,f} \\
& \frac{dCost_{Operational}}{dt}=m\cdot(Ca_0(t)-Ca(t))-4\cdot y_b \\
& \text{Interior point constraint } \forall T\in\{1,\ldots,100\} \\
& y_b-M\cdot y_{b,f}\le 0 \\
& \text{mpMPC}(t=T)-T_{c,T}=0 \\
& T(t)\le 450
\end{aligned}
\tag{16}
$$

The binary variable $y_{b,f}$ is introduced in the interior point constraints in order to account for the existence of the settling tank equipment only if y_b—corresponding to the operation of the tank—is active at any interior point. Since the latter is a piecewise constant variable if its value is one in at least one interval then the tank should exist. Therefore, an equipment cost associated with that is taken into account in the objective function. The temperature constraint is present to ensure the feasibility of the controller evaluation. The optimization results yield that the existence of the tank is necessary and operated until the concentration at the outlet of the CSTR approaches zero. The optimization results are presented below:

- CSTR Volume: $500\,\text{m}^3$
- $Ca_{0,nom}$: $10\,\text{mol/L}$
- $Ca_{0,dev}$: $5\,\text{mol/L}$
- m_{nom}: $7\,\text{m}^3/\text{s}$
- m_{dev}: $2\,\text{m}^3/\text{s}$

The tank is used at the start-up of the CSTR operation in order to normalize the concentration of the reactants until the controller can effectively manage the sinusoidal concentration deviation. It is clear that for different initial conditions ($Ca_{0,nom}$) the time period for which the tank is operated will vary. The initial concentration reported as optimal is by definition that concentration that would cause the greatest settling time to the CSTR operation. This is shown in Figures 5a, b

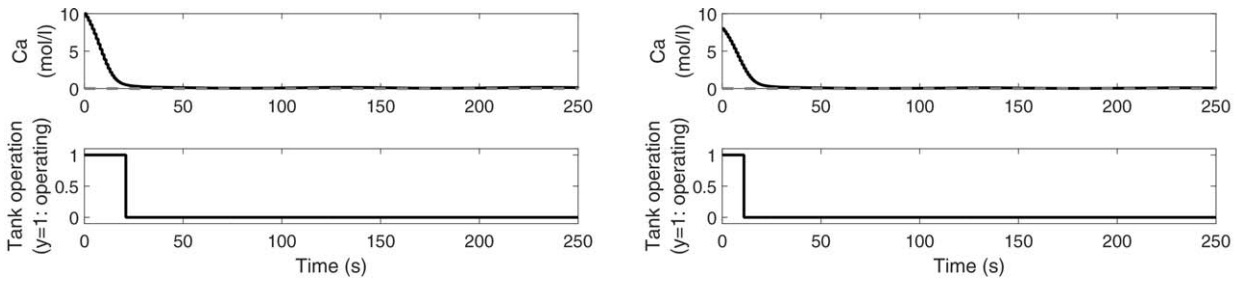

(a) Tank usage for a fixed initial $Ca_{0,nom} = 10mol/l$ (b) Tank usage for a fixed initial $Ca_{0,nom} = 8mol/l$. (Optimal).

Figure 5. Tank usage optimization results for fixed $Ca_{0,nom}$.

where the dynamic optimization has been repeated for a fixed $Ca_{0,nom}=8\,\mathrm{mol/L}$. The deviation from the optimal solution in the case where Ca_0 was fixed to 8 mol/L is 25.4%.

The Binary Distillation Column Example

The distillation column model describes the binary separation of benzene and toluene. The column is allowed a maximum number of trays to be 30 with no restriction on feed tray location. The purity in the top has a desired set point of 0.98 and the purity in the bottom has a desired setpoint of 0.02. The feed composition is assumed sinusoidal and is optimized similarly to the previous two examples.

"High fidelity" dynamic modeling

The distillation column utilizes mass and energy balances and thermodynamic relations to build the full model. The following assumptions have been made:

- Fast energy dynamics.
- Relative volatility.
- Constant molar hold up in condenser.
- Immediate pressure response.

Mass balances for each tray, reboiler, and condenser are used while assuming constant molar hold up in the total condenser. Energy balances are used in the reboiler and condenser while assuming an average temperature throughout the column. Relative volatility is used to determine vapor and liquid correlations in each tray and in the reboiler. The model assumes the reflux flow rate and the boil up rate to be the controllable variables in the system, and the molar hold ups to be the states of the system. Column diameter, reflux tray position, and feed tray position are the design variables, while the presence and position of the reboiler and condenser are fixed. Density of the liquid hold up on the trays is assumed to follow from a linear combination of the component densities.

The model of the binary distillation column is adapted from Ref. 131. The characteristic equations of the model are presented in 5 and in Appendix A, Table 1 for the nomenclature.

Antoine equations were used to determine vapor pressures at the top and bottom of the distillation column and the log-mean temperature approach was used for the heat exchange at the condenser and the reboiler. Since the "high-fidelity" model used here is a simplified model, the limiting constraints of the columns operation are expressed via thermodynamic limits which are manifested via the Antoine equations and subsequently the relative volatility relations. The distillation column is a multiple input multiple output system where the reflux flow rate and boil up flow rate are the degrees of freedom to the system, and the purity in the top and bottom is the output. The composition at the feed is treated as a disturbance to the system operation.

Model approximation

The high fidelity model of the distillation column consists of 50+ states and nonlinear equations. Random sets of I/O for different designs from the "high fidelity" model are introduced into the System Identification Toolbox in MATLAB® to acquire a linear state-space model of the form of Eq. 3. The identified state-space model is shown in Eq. 17.

$$\begin{aligned} x_{T+1} &= \begin{bmatrix} 0.9533 & -0.05507 \\ 0.0264 & 0.5494 \end{bmatrix} x_T + \begin{bmatrix} -0.01609 & -0.01346 \\ -0.1129 & 0.08987 \end{bmatrix} u_{c,T} + \\ &\quad \begin{bmatrix} -0.1257 & -9.703\cdot 10^{-5} & -4.163\cdot 10^{-4} \\ 1.005 & 7.184\cdot 10^{-4} & -5.874\cdot 10^{-5} \end{bmatrix} \begin{bmatrix} d_T \\ De \end{bmatrix} \\ y_T &= \begin{bmatrix} -0.2357 & -0.354 \\ 0.1098 & -0.4719 \end{bmatrix} x_T \\ T_s &= 1s \end{aligned} \tag{17}$$

where x_T are the identified states, $u_{c,T}$ are the reflux flow rate and the boil up rate, d_T is the composition of the feed, and De is the feed and reflux tray location. Note that the column diameter is correlated to the minimum vapor flow rate and therefore is the design decision of the system (see Eq. 18). Also note that the location of the trays are integer variables the handling of which in terms of multi-parametric programming will be discussed in the next section.

The step and impulse responses of the system are presented in Figures B3a, B3b, respectively.

Design of the multi-parametric model predictive controller

Similarly to the tank example in section the problem formulation is based on Eq. 4 and the tuning of the controller is presented in Table 6. Note that since the boil up flow rate is limited by the column diameter as presented in Eq. 18, the mpMPC is modified to account for the square of the column diameter as a design parameter. Note that since the column diameter is always greater than zero and it does not appear anywhere else within the mpMPC formulation we can define a new parameter $p=D_c^2$ which renders Eq. 18 linear inequality constraint.

$$0.4514\cdot V_B \le D_c^2 \tag{18}$$

The integer parameters corresponding to the tray locations are reformulated into binary parameters and solved based on the algorithm presented in Ref. 132. An alternative formulation could be the treatment of integer parameters as continuous parameters (similar to handling binary variables in Ref. 133) since the integer value realization of the parameter is a subset of their continuous values and the realization is not an mpMPC decision.

The objective of the design dependent controller is to maintain the purity set points for the top and bottom product at 98% vol and 2% vol regardless of the disturbance at the inlet of the system. Small deviations are allowed but penalized in the design optimization formulation.

Closed-loop validation

The validation step can be seen in Figure 6 where the controller is tested against the original high fidelity model. Note that the closed-loop validation needs to happen and be satisfactory for a range of different designs. Here we present the closed loop validation for a distillation column with the following characteristics:

- Condenser area: $100\,\mathrm{m}^2$.
- Reboiler area: $282.427\,\mathrm{m}^2$.
- Diameter of column: 1.9 m.
- Reflux tray position: 18.
- Feed tray position: 9.

Table 6. Weight Tuning for the mpMPC of the Distillation Column

MPC design parameters	Value
N	3
M	1
$QR_k, \forall k \in \{1,\ldots,\mathrm{N}\}$	$\begin{bmatrix} 10^7 & 0 \\ 0 & 10^7 \end{bmatrix}$
$R_k, \forall k \in \{1,\ldots,\mathrm{M}\}$	$\begin{bmatrix} 10^{-2} & 0 \\ 0 & 10^{-2} \end{bmatrix}$
x_{min}	$\begin{bmatrix} -10^3 & -10^3 \end{bmatrix}^T$
x_{max}	$\begin{bmatrix} 10^3 & 10^3 \end{bmatrix}^T$
u_{min}	$\begin{bmatrix} 2 & 3 \end{bmatrix}^T$
u_{max}	$\begin{bmatrix} 4.7 & 7 \end{bmatrix}^T$
y_{min}	$\begin{bmatrix} 0 & 0 \end{bmatrix}^T$
y_{max}	$\begin{bmatrix} 1 & 1 \end{bmatrix}^T$
d_{min}	$\begin{bmatrix} 0.45 & 1 & 1 \end{bmatrix}^T$
d_{max}	$\begin{bmatrix} 0.5 & 30 & 30 \end{bmatrix}^T$

Dynamic optimization

The dynamic optimization in Problem 10 is then formulated and solved allowing for the optimizer to select the optimal value for the area of the condenser, area of the reboiler, reflux tray location, feed tray location, and diameter of the column. To account for the reflux and feed tray location changing additional equations were added or modified as seen in Table 7.

Allowing the dynamic optimization to run over a time span of 1 h, the results obtained are presented in Table 8.

It can be seen that by utilizing the simultaneous design and control approach presented here, a distillation column with a smaller annualized total cost is designed.

The Domestic Cogeneration Unit Example

The domestic internal combustion engine powered cogeneration example of Refs. 134,135 is used here. For the domestic cogeneration unit we assume the possibility of a dual mode of operation, i.e., the unit can either follow an electricity demand (Mode 1 operation) or a hot water demand (Mode 2 operation) based on cost of operation criteria. The decentralized control schemes for this purpose are described in Ref. 134 in detail. The unit is assumed to provide heat and power to an area connected to the electricity and natural gas grid, therefore, any power that the unit cannot cover are covered by the grid, at a cost.** Similarly surplus of electrical power is provided to the grid, at a revenue and heat in the form of water discarded at a cost. The design aspect is the size of the internal combustion engine. Indicatively, a larger engine can potential cover greater demands but requires a greater investment cost. Conversely, a smaller engine might be less cost effective in the long term operation of the plant. A sinusoidal demand for electrical power and hot water is assumed. Previously we presented a similar example with Mode 1 operation where the simultaneous design and control employed PI controllers and later a mpMPC was formulated to fit the optimal design.[136,137] Here, we formulate the explicit controllers to be design

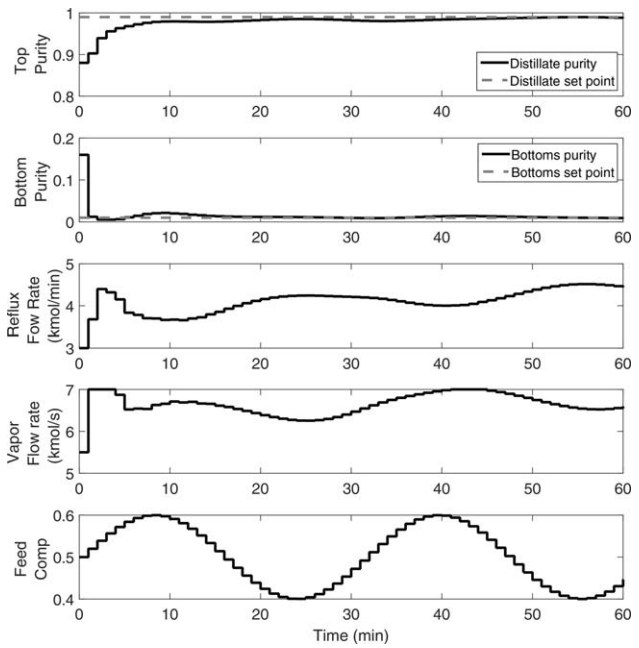

Figure 6. Closed loop validation of the controller against the high fidelity model.

Table 7. Additional/Modified Equations for Dynamic Optimization

Description	Equation
Feed tray location	$F_k = F\delta_k^f,\ \sum_{k=1}^{Ntrays} \delta_k^f = 1$
Reflux tray location	$R_k = R\delta_k^r,\ \sum_{k=1}^{Ntrays} \delta_k^r = 1$
Feed tray location only below reflux	$\delta_k^f - \sum_{k\prime=k}^{Ntrays} \delta_{k\prime}^r \le 0$
Component mass balance	$\left(\sum_{k\prime=k}^{Ntrays} \delta_{k\prime}^r\right) \frac{dM_{i,k}}{dt} = L_{k+1}x_{i,k+1} + V_{k-1}y_{i,k-1} + F_k z_{i,f} + R_k x_{i,d} - L_k x_{i,k} - V_k y_{i,k},\ \forall k \in \{2..,Ntrays-1\}$
Total mass balance	$\left(\sum_{k\prime=k}^{Ntrays} \delta_{k\prime}^r\right) \frac{dM_k}{dt} = L_{k+1} + V_{k-1} + F_k + R_k - L_k - V_k,\ \forall k \in \{2..,Ntrays-1\}$
Reboiler cost	$C_{reb} = 0.6 \cdot 101.3 \frac{M\&S}{280} \left(\frac{10^4 A_R}{144 \cdot 2.54^2}\right)^{0.65} \cdot 3.22 \cdot 1.35$
Total cost	$TotalCost = OpCost + \frac{1}{3}(C_{column} + C_{reb} + C_{cond})$

Component i is benzene, tray number is $k \in \{1\ldots Ntrays\}$ unless stated otherwise.

Table 8. Results of the Current Approach and Comparison with Ref. 131

	Current approach	Comparison with Ref. 131
Condenser area (m^2)	120	132
Reboiler area (m^2)	266	276
Diameter of column (m)	1.62	1.65
Reflux tray	25	25
Feed tray	12	12
Total cost (k$)	590	620

**The cost of electrical power fluctuates between night time and day time which is taken into account in this example.

Table 9. Residential CHP Model Overview

Description	Equation
Throttle valve—fuel and air manipulation	$\dot{m}_{th}=c_d A_{th}\frac{P_{ab}}{\sqrt{R_\beta T_{ab}}}\psi\left(\frac{P_{ab}}{P_{mn}}\right)$
Manifolds—pressure difference driven flow for the inlet air and exhaust gases	$\frac{d}{dt}m_{mn}=\dot{m}_{mn,in}-\dot{m}_{mn,out}$
	$\dot{V}_{mn,out}=cpf\left(P_{mn}-P_{mn,out}\right)$
	$\dot{V}_{mn}\frac{d}{dt}E=\dot{m}_{mn,in}h_{mn,in}-\dot{m}_{mn,out}h_{mn,out}$
Internal combustion engine—energy and mass balances	$\dot{m}_{ex}=\frac{P_{mn}}{R_\beta T_{mn}}\frac{V_d}{4\pi}\eta_{vl}\omega_{en}$
	$\dot{m}_{mn,out}\left(h_{mn,out}+\sum_{i=aircomp.}\left(x_{air,i}h^o_{f,air,i}\right)\right)$
	$+\dot{m}_\phi\left(h_\phi+\sum_{j=fuelcomp.}\left(x_{\phi,j}h^o_{f,fuel,j}\right)\right)$
	$-\dot{m}_{ex}\left(h_{ex}+\sum_{k=exhaustcomp.}\left(x_{ex,k}h^o_{f,ex,k}\right)\right)$
	$=\dot{Q}_f+\dot{Q}_{cg\to cw}+\dot{W}_c+\dot{W}_{en}$
Crankshaft—Torque generation	$To_{en}=\frac{P_{meb}V_d}{4\pi}$
Generator—power generation through torque	$\frac{d}{dt}To_{cl}=\frac{1}{Fl}(To_{en}-To_{cl})$
	$Pec=\eta_{en}To_{cl}\omega_{en}$
Engine cooling system—energy balances	$\frac{d}{dt}T_i=\frac{\dot{Q}_{in,i}-\dot{Q}_{out,i}}{m_i c_{p,i}}$
	$\forall i\in$ engine cooling system components
	$\dot{Q}_{a\to b}=TC_{ab}A_{ab}(T_a-T_b)$
	$\forall a,b\in$ engine cooling system components
Heat exchangers—energy balances	$Q=UA\Delta T_{mean}$
	$\Delta T_{mean}=\frac{\Delta T_{in}-\Delta T_{out}}{log\left(\left\lvert\frac{\Delta T_{in}}{\Delta T_{out}}\right\rvert\right)}$

dependent, similarly to the three previous examples and proceed with a dynamic design optimization.

"High fidelity" dynamic modeling

The high "fidelity model" of the cogeneration unit features the interactions of each component of the unit. It is based on first principles and correlations and is a non-linear DAE system with 379 equations, 15 of which are differential, and 6 degrees of freedom. An overview is presented in Table 9 and Table 2. The full model can be found in Ref. 135.

The necessity of the model approximation and the decentralization of such a system lies with the fact that (1) its complexity would pose a significant challenge for advanced optimization techniques and (2) the different modes of operation require advanced control schemes as explained in Ref. 134. The latter can be comprehended by the fact that the process is multi-product, as it is able to produce simultaneously usable heat and power. The dependence between heat and power generation although, makes it impossible to produce both of them simultaneously at the desired level, at all times.

The CHP unit is treated as the interactions of the heat generation subsystem with the power generation subsystem.[134] The power generation subsystem is design dependent as the amount of power generated from the unit is directly affected by the size of the internal combustion engine. The heat recovery subsystem is dependent on the power generation, as it correlates the amount of hot water produced and its temperature to the operating level of the power generation subsystem. Treating the power generation level as a known disturbance (in the case of Mode 1 operation) or as a projected operating level set point (in the case of Mode 2 operation) results only into an indirect design correlation. Therefore, we proceed here considering only the directly affected design dependent power generation subsystem. The formulation for the heat recovery subsystem follows exactly the principles presented in Ref. 134.

Model approximation

The approximate model for the power generation subsystems is identified via System Identification in MATLAB®. In order for this to happen, I/O data for a range of different designs are introduced. The input to the system is the opening of the throttle valve which manipulates the amount of air and fuel that enters the combustion chambers of the internal combustion engine. Based on the size of the engine (treated here as a measured disturbance), the power output is affected as shown in Eq. 19. The state-space model for the heat recovery subsystem is presented in Eq. 20.

$$\begin{aligned} x_{T+1}&=0.9799\cdot x_T+0.006328\cdot u_{c,T}+6.516\cdot De\\ y_T&=7.839\cdot x_T\\ T_s&=0.1s \end{aligned} \tag{19}$$

where x_T are the identified states, $u_{c,T}$ is the throttle valve opening, d_T and De is the volume of the internal combustion engine. The output y_T is the electrical power generated via the subsystem.

$$\begin{aligned} x_{T+1}&=\begin{bmatrix} 0.997 & 0.1026 & -0.002958\\ -0.001527 & 0.9404 & 0.1663\\ -0.05827 & -0.05636 & 0.179 \end{bmatrix}\cdot x_T\\ &+\begin{bmatrix} -0.007864 & 0.001107\\ 0.2801 & -0.03306\\ -1.28 & 0.1464 \end{bmatrix}\cdot u_{c,T}\\ y_T&=\begin{bmatrix} -529.9 & -2.827 & 0.2521 \end{bmatrix}\cdot x_T\\ T_s&=0.1s \end{aligned} \tag{20}$$

where x_T are the identified states and $u_{c,T}$ are the power generation level and water flow rate in the heat recovery subsystem. The output y_T is the temperature of the hot water at the outlet of the system. Note that depending on the mode of operation of the CHP system one of the inputs is treated as a measured disturbance to the system (i.e., the power generation level is treated as a measured disturbance in Mode 1 and the water flow rate is treated as a measured disturbance in Mode 2).

Table 10. Weight Tuning for the mpMPC of the CHP Unit

MPC design parameters	Value
N	3
M	3
$QR_k, \forall k \in \{1,\ldots,\mathrm{N}\}$	31.25
$R1_k, \forall k \in \{1,\ldots,\mathrm{M}\}$	0.1
x_{min}	0
x_{max}	5
u_{min}	0.01
u_{max}	1
y_{min}	0
y_{max}	11
d_{min}	1500
d_{max}	5000
Δu_{min}	−0.1
Δu_{max}	0.1

The step and impulse responses of the entire system are presented in Figures B4a, B4b, respectively.

Design of the multi-parametric model predictive controller

The multi-parametric model predictive controller problem (based on Eq. 4) is formulated and solved with POP.[117] The tuning of the controller is presented in Table 10. The tuning of the controllers for the heat recovery subsystem is omitted here as it has been presented previously and is identical to Ref. 134.

Note the following:

- The minimum value of the throttle valve opening is not equal to 0. This means that there is a minimum operating level for the CHP unit and that we do not account for the system ability to switch off as part of the control strategy.
- The maximum output is linearly correlated to the size of the internal combustion engine based on the function $y_{max}=0.0011 \cdot De+4.5148$, where y_{max} is the maximum power output in $\times 10kW$ and De is the internal combustion engine volume (treated in the context of mpMPC as the disturbance d).

In Mode 1, the control scheme attempts to (1) cover the electrical power demand and (2) produce water of a predefined temperature, regardless of the flow rate. In Mode 2, the control scheme attempts to produce hot water of (1) a predefined flow rate an (2) temperature, regardless of the operating level of the power generation subsystem. The most important limiting factor for the controller performance of the CHP system is to guarantee that there exist no violation of the water temperature above 100°C due to a possible overshoot. Further information regarding this can be found in Ref. 134.

Closed-loop validation

Closing the loop of the CHP system involves both operating modes. In Figure 7 the simulation presents a power driven operation for the first 120 s and the last 50 s. A heat recovery driven operation is shown for time between 120 and 300 s. The simulation follows a variable electrical power and hot water flow rate demand. It is assumed that the hot water temperature at the outlet is 70°C. The design of the internal combustion engine for this operation is 1500 cc.

In Figures 8 and 9 present the response of the Mode 1 and Mode 2 control scheme, respectively, for different designs. Note that the same design dependent controller is used for different closed-loop simulations. Despite that, the different designs cause a different response to the system. For example, the throttle valve opening is different between the different designs which leads to different fuel consumption therefore to different operating cost of the CHP unit. Although the difference is relatively small (i.e., the characteristics of the overall profile are similar) those differences suffice to affect the long

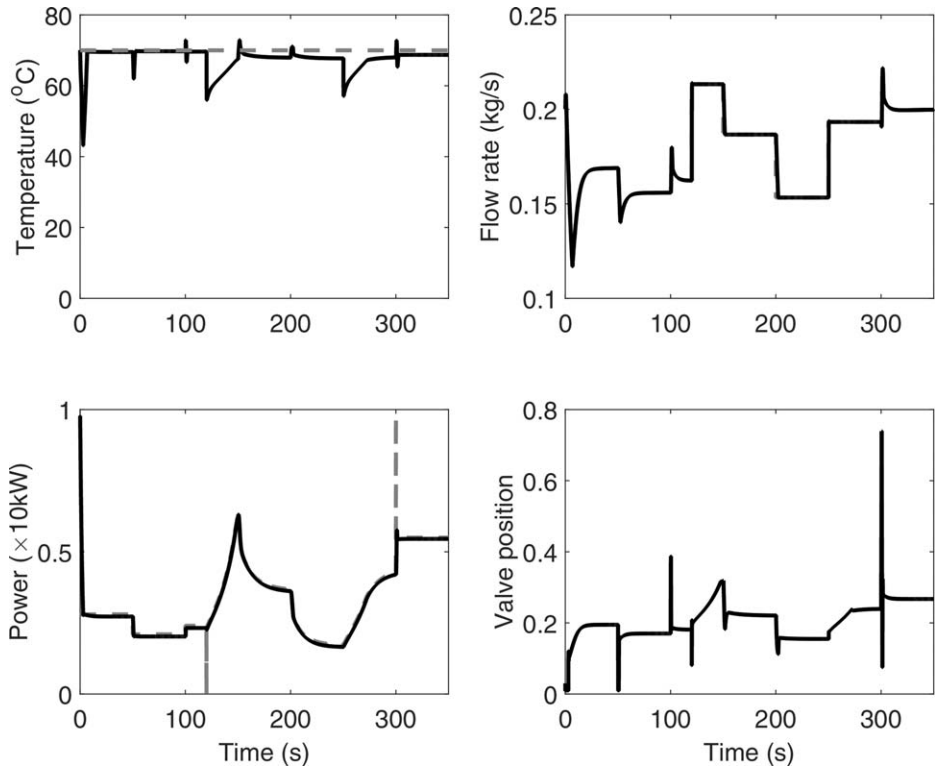

Figure 7. Closed loop validation of the controller against the high fidelity model.

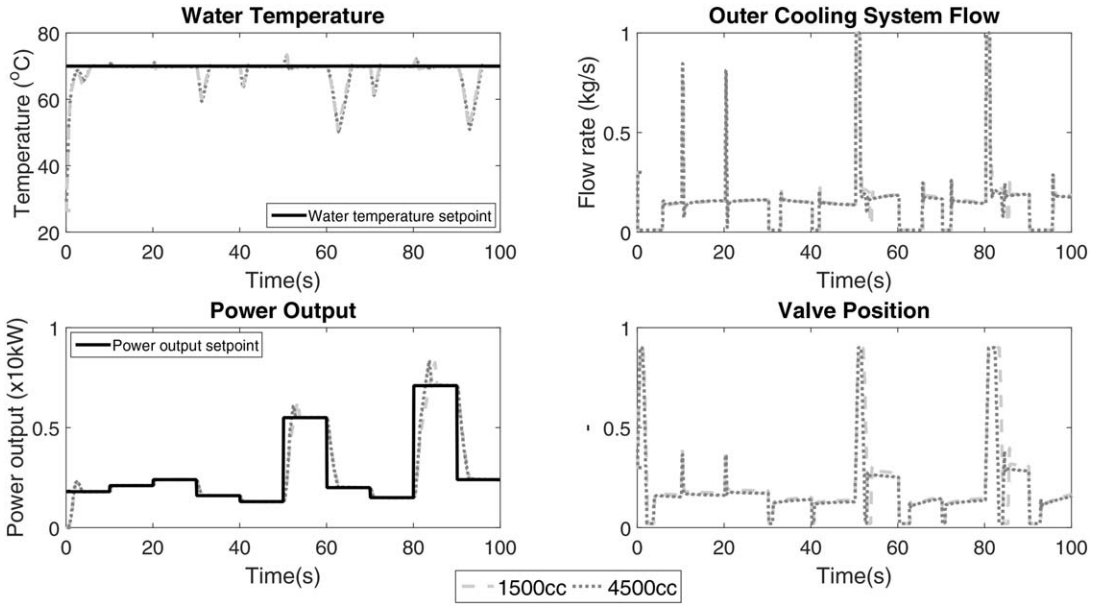

Figure 8. Design dependent mpMPC—Mode 1.

term operating cost of the unit. The more intense operation of the smaller engine in comparison with the less intense operation of the larger engine is a clear trade-off between investments and operational cost, an aspect that the optimal design takes into account. Table 11 shows a snapshot of the explicit actions for an engine size of 1500 cc and Table 12 for an engine size of 4500 cc. The upper graphs within Tables 11 and 12 show the optimal action $u_{c,T}$ applied to the system as a function of the approximate states x_T while the lower graphs the critical region that corresponds to that action. The expressions of the control actions that correspond to the same critical region are identical for different designs. The effect of the different designs to the optimal action is visible from the fact that for actions corresponding to the same critical region the numerical value that is ultimately applied to the system is different.

Figure 10 represents a snapshot of the power generation of the CHP system for different designs under a fixed power demand step change scenario. More specifically, the different responses of the system (y_T) are plotted against the optimal actions ($u_{c,T}$) for three different designs of the internal combustion engine volume (De). This shows that although an advanced design dependent control scheme has been employed there still exists a difference between the closed loop response of the system when $y_T(u_{c,T})$ is regarded.

Dynamic optimization

The dynamic optimization formulation for the CHP system is similar to the previous three examples. More specifically, a sinusoidal demand is introduced for both the electrical power and hot water flow rate while the temperature for the hot water

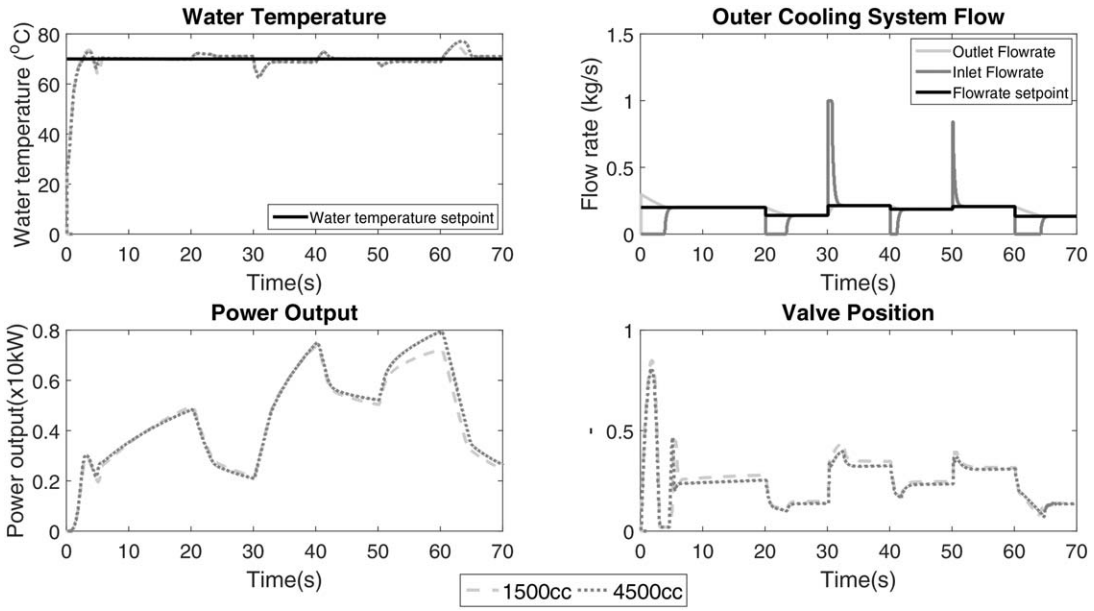

Figure 9. Design dependent mpMPC—Mode 2.

Table 11. Optimal Action as a Function of the Parameters and Design Variable (De=1500cc)

$u_c^{1500}=f(\theta,De)$		
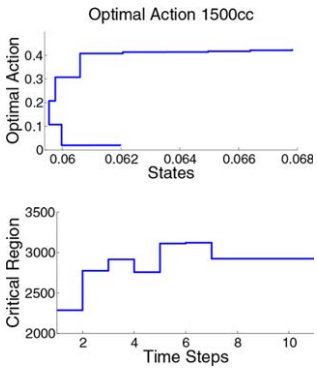	$CR_{T=1}=2287$	$u_{c,T=1}^{1500}=0.02$
	$CR_{T=2}=2775$	$u_{c,T=2}^{1500}=0.02$
	$CR_{T=3}=2915$	$u_{c,T=3}^{1500}=3.05x_T+0.0351u_{c,T=2}^{1500}-9.89\cdot10^{-6}De-14.81y_T+14.81y_T^{SP}$
	$CR_{T=4}=2757$	$u_{c,T=4}^{1500}=u_{c,T=3}^{1500}+0.1$
	$CR_{T=5}=3112$	$u_{c,T=5}^{1500}=u_{c,T=4}^{1500}+0.1$
	$CR_{T=6}=3122$	$u_{c,T=6}^{1500}=u_{c,T=5}^{1500}+0.1$
	$CR_{T=7}=2924$	$u_{c,T=7}^{1500}=3.15x_T+0.004u_{c,T=6}^{1500}-1.02\cdot10^{-5}De-7.9y_T+7.9y_T^{SP}+0.0849$
	$CR_{T=8}=2924$	$u_{c,T=8}^{1500}=3.15x_T+0.004u_{c,T=7}^{1500}-1.02\cdot10^{-5}De-7.9y_T+7.9y_T^{SP}+0.0849$
	$CR_{T=9}=2924$	$u_{c,T=9}^{1500}=3.15x_T+0.004u_{c,T=8}^{1500}-1.02\cdot10^{-5}De-7.9y_T+7.9y_T^{SP}+0.0849$
	$CR_{T=10}=2924$	$u_{c,T=10}^{1500}=3.15x_T+0.004u_{c,T=9}^{1500}-1.02\cdot10^{-5}De-7.9y_T+7.9y_T^{SP}+0.0849$

Table 12. Optimal Action as a Function of the Parameters and Design Variable (De=4500cc)

$u_{c,T}^{4500}=f(\theta,De)$		
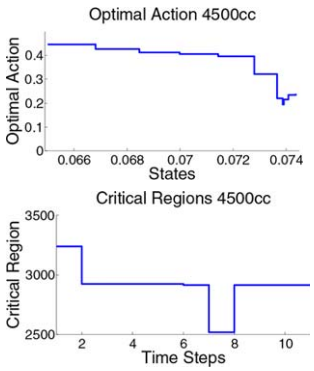	$CR_{T=1}=3239$	$u_{c,T=1}^{4500}=u_{opt}^{T=0}+0.1$
	$CR_{T=2}=2924$	$u_{c,T=2}^{4500}=3.15x_T+0.004u_{c,T=1}^{4500}-1.02\cdot10^{-5}De-7.9y_T+7.9y_T^{SP}+0.0849$
	$CR_{T=3}=2924$	$u_{c,T=3}^{4500}=3.15x_T+0.004u_{c,T=2}^{4500}-1.02\cdot10^{-5}De-7.9y_T+7.9y_T^{SP}+0.0849$
	$CR_{T=4}=2924$	$u_{c,T=4}^{4500}=3.15x_T+0.004u_{c,T=3}^{4500}-1.02\cdot10^{-5}De-7.9y_T+7.9y_T^{SP}+0.0849$
	$CR_{T=5}=2924$	$u_{c,T=5}^{4500}=3.15x_T+0.004u_{c,T=4}^{4500}-1.02\cdot10^{-5}De-7.9y_T+7.9y_T^{SP}+0.0849$
	$CR_{T=6}=2915$	$u_{c,T=6}^{4500}=3.04x_T+0.04u_{c,T=5}^{4500}-9.85\cdot10^{-6}De-14.81y_T+14.81y_T^{SP}$
	$CR_{T=7}=2519$	$u_{c,T=7}^{4500}=u_{c,T=6}^{4500}-0.1$
	$CR_{T=8}=2915$	$u_{c,T=8}^{4500}=3.04x_T+0.04u_{c,T=7}^{4500}-9.85\cdot10^{-6}De-14.81y_T+14.81y_T^{SP}$
	$CR_{T=9}=2915$	$u_{c,T=9}^{4500}=3.04x_T+0.04u_{c,T=8}^{4500}-9.85\cdot10^{-6}De-14.81y_T+14.81y_T^{SP}$
	$CR_{T=10}=2915$	$u_{c,T=10}^{4500}=3.04x_T+0.04u_{c,T=9}^{4500}-9.85\cdot10^{-6}De-14.81y_T+14.81y_T^{SP}$

is maintained at 70°C. The pricing for the electrical power fluctuates between a high value during the day and a low value during the night time. The purpose of the dynamic optimization problem in this case is dual:

- The determination of the size of the internal combustion engine of the CHP.
- The determination of the operating mode of the system for a given demand scenario and pricing scheme.

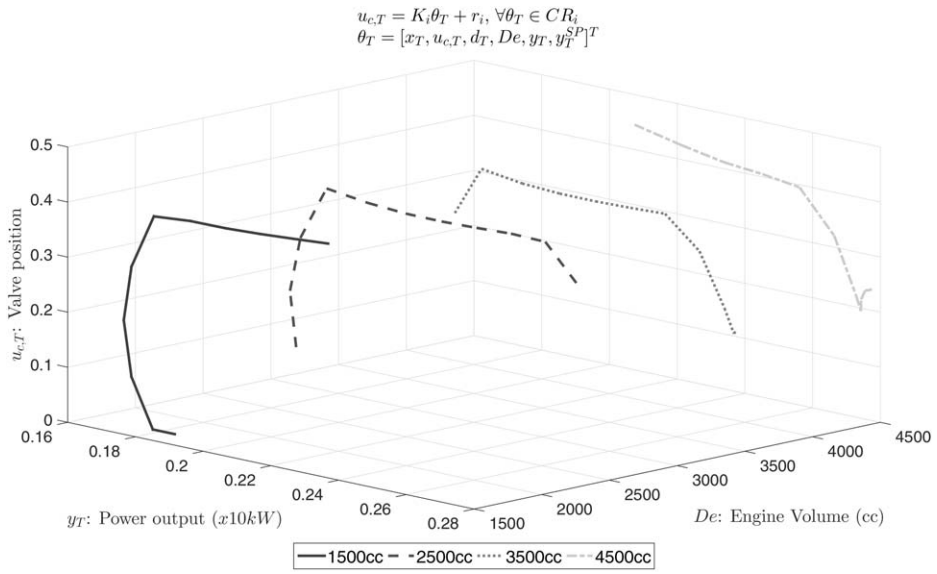

Figure 10. Design dependent mpMPC—state and optimal action propagation for different designs.

Table 13. Computational Time Statistics

Case study	Time scale	
	(MI)DO problem	mpMPC offline problems
Simple tank	<1 min	<5 min
CSTR	<10 min	<5 min
Distillation column	<2 h	<10 min
CHP	<12 h	<1 h (for all problems combined)

The objective function is formulated as a Total cost function that includes (1) the investment cost of the CHP, (2) the operating cost of the unit as a function of the amount of fuel required for electrical power and heat production, (3) the cost of external resources required to cover possible demand shortages, (4) the cost of discarding surplus heat (in the form of hot water), and (5) the revenues from selling surplus power to the grid.

The MIDO algorithm converges to the an operation based on the day and night pricing of electrical power, i.e., the system prefers to operate on a power production driven operation during the day when the electricity price is higher and revert to a heat generation driven demand during night time. Furthermore, the size of the internal combustion engine converges to 2203 cc, a value that does not correspond to the upper or lower bound of the design variable. It is clear through testing several demand scenarios (and from previous studies[137]) that the operating mode of the system is primarily a matter of fuel and electricity price. More specifically, the choice for the operating mode of the CHP system, although here optimized for a given demand scenario and electricity price scheme, is a matter that needs to be determined as the fluctuation in demand and pricing happens. Therefore, this is a matter of an economic/operational optimization for demand side uncertainty, such as a scheduling formulation as described in Ref. 1.

Computational Statistics and Requirements

All computational experiments were performed on a computer running Windows 7 Enterprise, SP1, MATLABR2015b® 64bit, gPROMS® 4.2 64bit and Visual Studio 2012. The computer was equipped with 16 GB of RAM and Intel® Core™i7–4790 clocked at 3.60GHz.

The computational time scales for the mpMPC and MIDO problems are reported in Table 13.

Concluding Remarks

We presented a framework for the application of design and control optimization via multi-parametric programming although four case studies. Through the formulation of a DO with mpMPC where we ensure cyclic operation we determined the size of a simple tank. The size of a CSTR was determined via the formulation of a design MIDO and a corresponding multi-parameric controller. In that case, the possibility of adding a settling tank was also considered. The binary distillation column example was revisited and the size, and key tray locations were determined via a design MIDO formulation and mpMPC with the latter taking into account discrete alternatives. The common basis for these three examples is that the operation of the aforementioned equipment focuses on a simple objective. In the case of the tank the operating objective is to maintain a volume set point. The CSTR attempts to produce as much product as possible with a temperature constraint and the distillation column aims to achieve a certain purity level.

On the contrary to the previous three examples the case of the CHP is different in the sense that its operation is variable, i.e., the system should be able to follow different operating set points at different times. Although a simultaneous design and control approach provides great insight regarding its operation, particularly the change between operating modes within the day, it is not able to determine the long term operation of the system efficiently. In other words, a decision about a long term characteristic (such as the size of the internal combustion engine) of a variably operating system (alternating operating set points) cannot be made without considering the optimality of the aforementioned set points, especially in a case of a multi-product process. Therefore, subject of our current work is the simultaneous consideration of the optimality of the set points based on midterm financial criteria, i.e., the inclusion of simultaneous reactive scheduling formulations of such systems.

Acknowledgments

Financial support from Texas A&M University, Texas A&M Energy Institute and EPSRC (EP/M027856/1) is gratefully acknowledged.

Literature Cited

1. Pistikopoulos EN, Diangelakis NA. Towards the integration of process design, control and scheduling: Are we getting closer? *Comput Chem Eng*. 2016;91:85–92.
2. Pistikopoulos EN, Ierapetritou MG. Novel approach for optimal process design under uncertainty. *Comput Chem Eng*. 1995;19(10):1089–1110.
3. Ricardez-Sandoval LA. Optimal design and control of dynamic systems under uncertainty: a probabilistic approach. *Comput Chem Eng*. 2012;43:91–107.
4. Flores-Tlacuahuac A, Biegler LT. Simultaneous mixed-integer dynamic optimization for integrated design and control. *Comput Chem Eng*. 2007;31(5–6):588–600.
5. Alvarado-Morales M, Hamid MKA, Sin G, Gernaey KV, Woodley JM, Gani R. A model-based methodology for simultaneous design and control of a bioethanol production process. *Comput Chem Eng*. 2010;34(12):2043–2061.
6. Skogestad S, Morari M. Control configuration selection for distillation columns. *AIChE J*. 1987;33(10):1620–1635.
7. Narraway LT, Perkins JD, Barton GW. Interaction between process design and process control: economic analysis of process dynamics. *J Process Contr*. 1991;1(5):243–250.
8. Bogle IDL, Rashid M. An assessment of dynamic operability measures. *Comput Chem Eng*. 1989;13(11–12):1277–1282.
9. Fraga ES, Hagemann J, Estrada-Villagrana A, Bogle IDL. Incorporation of dynamic behaviour in an automated process synthesis system. *Comput Chem Eng*. 2000;24(2–7):189–194.
10. Papalexandri KP, Pistikopoulos EN. Synthesis and retrofit design of operable heat exchanger networks. 1.flexibility and structural controllability aspects. *Ind Eng Chem Res*. 1994;33(7):1718–1737.
11. Mohideen MJ, Perkins JD, Pistikopoulos EN. Robust stability considerations in optimal design of dynamic systems under uncertainty. *J Process Contr*. 1997;7(5):371–385.
12. Georgiadis M, Schenk C, Gani MR, Pistikopoulos EN. The interactions of design, control and operability in reactive distillation systems. *Comput Aid Chem Eng*. 2001;9(C):997–1002.
13. Luyben ML, Floudas CA. Analyzing the interaction of design and control-1: a multiobjective framework and application to binary distillation synthesis. *Comput Chem Eng*. 1994;18(10):933–969.
14. Floudas CA. Global optimization in design and control of chemical process systems. *J Process Contr*. 2000;10(2):125–134.
15. Floudas CA, Gümüş ZH, Ierapetritou MG. Global optimization in design under uncertainty: feasibility test and flexibility index problems. *Ind Eng Chem Res*. 2001;40(20):4267–4282.

16. Bahri PA, Bandoni JA, Romagnoli JA. Integrated flexibility and controllability analysis in design of chemical processes. *AIChE J*. 1997;43(4):997–1015.
17. Chawankul N, Ricardez-Sandoval LA, Budman H, Douglas PL. Integration of design and control: A robust control approach using mpc. *Canad J Chem Eng*. 2007;85(4):433–446.
18. Sánchez-Sánchez K, Ricardez-Sandoval L. Simultaneous process synthesis and control design under uncertainty: a worst-case performance approach. *AIChE J*. 2013;59(7):2497–2514.
19. Fisher WR, Doherty MF, Douglas JM. Interface between design and control. 1. Process controllability. *Ind Eng Chem Res*. 1988; 27(4):597–605.
20. Fisher WR, Doherty MF, Douglas JM. Interface between design and control. 2. Process operability. *Ind Eng Chem Res*. 1988;27(4): 606–611.
21. Fisher WR, Doherty MF, Douglas JM. Interface between design and control. 3. Selecting a set of controlled variables. *Ind Eng Chem Res*. 1988;27(4):611–615.
22. Skogestad S, Morari M. Design of resilient processing plants-ix. Effect of model uncertainty on dynamic resilience. *Chem Eng Sci*. 1987;42(7):1765–1780.
23. ChatrattanawetSkogestad NS, Arpornwichanop A. Control structure design and controllability analysis for solid oxide fuel cell. *Chem Eng Trans*. 2014;39(Special Issue):1291–1296.
24. Close EJ, Salm JR, Bracewell DG, Sorensen E. A model based approach for identifying robust operating conditions for industrial chromatography with process variability. *Chem Eng Sci*. 2014;116: 284–295.
25. Gevelber, MA, Stephanopoulos, G. Control and system design for the czochralski crystal growth process. In: *American Society of Mechanical Engineers, Dynamic Systems and Control Division (Publication) DSC*, *Vol*. 9, 1988: 35–40.
26. Banerjee I, Ierapetritou MG. Design optimization under parameter uncertainty for general black-box models. *Ind Eng Chem Res*. 2002;41(26):6687–6697.
27. Gong J, Hytoft G, Gani R. An integrated computer aided system for integrated design and control of chemical processes. *Comput Chem Eng*. 1995;19(Suppl. 1):489–494.
28. Figueroa JL, Bahri PA, Bandoni JA, Romagnoli JA. Economic impact of disturbances and uncertain parameters in chemical processes—a dynamic back-off analysis. *Comput Chem Eng*. 1996; 20(4):453–461.
29. Vega P, Lamanna R, Revollar S, Francisco M. Integrated design and control of chemical processes—part ii: an illustrative example. *Comput Chem Eng*. 2014;71:618–635.
30. Soroush M, Kravaris C. Optimal design and operation of batch reactors. 2. A case study. *Ind Eng Chem Res*. 1993;32(5):882–893.
31. Soroush M, Kravaris C. Optimal design and operation of batch reactors. 1. Theoretical framework. *Ind Eng Chem Res*. 1993;32(5): 866–881.
32. Bansal V, Perkins JD, Pistikopoulos EN, Ross R, Van Schijndel JMG. Simultaneous design and control optimisation under uncertainty. *Comput Chem Eng*. 2000;24(2–7):261–266.
33. Bansal V, Ross R, Perkins JD, Pistikopoulos EN. Interactions of design and control: double-effect distillation. *J Process Contr*. 2000;10(2):219–227.
34. Bansal V, Perkins JD, Pistikopoulos EN. A case study in simultaneous design and control using rigorous, mixed-integer dynamic optimization models. *Ind Eng Chem Res*. 2002;41(4):760–778.
35. Georgiadis MC, Schenk M, Pistikopoulos EN, Gani R. The interactions of design, control and operability in reactive distillation systems. *Comput Chem Eng*. 2002;26(4–5):735–746.
36. Bansal V, Sakizlis V, Ross R, Perkins JD, Pistikopoulos EN. New algorithms for mixed-integer dynamic optimization. *Comput Chem Eng*. 2003;27(5):647–668.
37. Washington ID, Swartz CLE. Design under uncertainty using parallel multiperiod dynamic optimization. *AIChE J*. 2014;60(9):3151–3168.
38. Sakizlis V, Perkins JD, Pistikopoulos EN. Parametric controllers in simultaneous process and control design optimization. *Ind Eng Chem Res*. 2003;42(20):4545–4563.
39. Sakizlis V, Perkins JD, Pistikopoulos EN. Parametric controllers in simultaneous process and control design. *Comput Aid Chem Eng*. 2003;15(C):1020–1025.
40. Sakizlis V, Perkins JD, Pistikopoulos EN. Recent advances in optimization-based simultaneous process and control design. *Comput Chem Eng*. 2004;28(10):2069–2086.
41. V, Sakizlis JD, Perkins EN. Pistikopoulos Chapter b1 simultaneous process and control design using mixed integer dynamic optimization and parametric programming. *Comput Aid Chem Eng*. 2004; 17(C):187–215.
42. Noeres C, Dadhe K, Gesthuisen R, Engell S, Górak A. Model-based design, control and optimisation of catalytic distillation processes. *Chem Eng Process Process Intensif*. 2004;43(3):421–434.
43. Malcolm A, Polan J, Zhang L, Ogunnaike BA, Linninger AA. Integrating systems design and control using dynamic flexibility analysis. *AIChE J*. 2007;53(8):2048–2061.
44. Flores-Tlacuahuac A, Biegler LT. Integrated control and process design during optimal polymer grade transition operations. *Comput Chem Eng*. 2008;32(11):2823–2837.
45. Brengel DD, Seider WD. Coordinated design and control optimization of nonlinear processes. *Comput Chem Eng*. 1992;16(9):861–886.
46. Ricardez-Sandoval LA, Budman HM, Douglas PL. Simultaneous design and control of processes under uncertainty: a robust modelling approach. *J Process Contr*. 2008;18(7–8):735–752.
47. Mehta S, Ricardez-Sandoval LA. Integration of design and control of dynamic systems under uncertainty: a new back-off approach. *Ind Eng Chem Res*. 2016;55(2):485–498.
48. Rafiei-Shishavan M, Mehta S, Ricardez-Sandoval LA. Simultaneous design and control under uncertainty: A back-off approach using power series expansions. *Comput Chem Eng*. 2017;99:66–81.
49. Mohideen MJ, Perkins JD, Pistikopoulos EN. Optimal synthesis and design of dynamic systems under uncertainty. *Comput Chem Eng*. 1996;20(Suppl. 2):S895–S900.
50. Kookos IK, Perkins JD. An algorithmic method for the selection of multivariable process control structures. *J Process Contr*. 2002; 12(1):85–99.
51. Kookos IK, Perkins JD. Chapter b2 the back-off approach to simultaneous design and control. *Comput Aid Chem Eng*. 2004;17(C): 216–238.
52. Kookos IK, Perkins JD. Control structure selection based on economics: generalization of the back-off methodology. *AIChE J*. 2016;62(9):3056–3064.
53. De La Fuente RL-N, Flores-Tlacuahuac A. Integrated design and control using a simultaneous mixed-integer dynamic optimization approach. *Ind Eng Chem Res*. 2009;48(4):1933–1943.
54. Li X, Tomasgard A, Barton, PI. Decomposition strategy for natural gas production network design under uncertainty. In *Proceedings of the IEEE Conference on Decision and Control*, 2010:188–193.
55. Chen Y, Adams TA, Barton PI. Optimal design and operation of flexible energy polygeneration systems. *Ind Eng Chem Res*. 2011; 50(8):4553–4566.
56. Chen Y, Adams TA, Barton PI. Optimal design and operation of static energy polygeneration systems. *Ind Eng Chem Res*. 2011; 50(9):5099–5113.
57. Li X, Barton PI. Optimal design and operation of energy systems under uncertainty. *J Process Contr*. 2015;30:1–9.
58. Ghobeity A, Mitsos A. Optimal design and operation of a solar energy receiver and storage. *J Solar Energ Eng Transact ASME*. 2012;134(3).
59. Zhang L, Xue C, Malcolm A, Kulkarni K, Linninger AA. Distributed system design under uncertainty. *Ind Eng Chem Res*. 2006; 45(25):8352–8360.
60. Li H, Gani R, Jørgensen SB. Integration of design and control for energy integrated distillation. *Comput Aid Chem Eng*. 2003;14(C): 449–454.
61. Ramírez E, Gani R. Design and control structure integration from a model-based methodology for reaction-separation with recycle systems. *Comput Aid Chem Eng*. 2005;20(C):1519–1524.
62. Hamid MKA, Sin G, Gani R. Integration of process design and controller design for chemical processes using model-based methodology. *Comput Chem Eng*. 2010;34(5):683–699.
63. Georgis D, Jogwar SS, Almansoori AS, Daoutidis P. Design and control of energy integrated sofc systems for in situ hydrogen production and power generation. *Comput Chem Eng*. 2011;35(9): 1691–1704.
64. Lee HH, Koppel LB, Lim HC. Integrated approach to design and control of a class of countercurrent processes. *Ind Eng Chem Process Des Dev*. 1972;11(3):376–382.
65. Hsu K-Y, Hsiao Y-C, Chien I-L. Design and control of dimethyl carbonate-methanol separation via extractive distillation in the dimethyl carbonate reactive-distillation process. *Ind Eng Chem Res*. 2010;49(2):735–749.

66. Gunasekaran S, Mancini ND, Mitsos A. Optimal design and operation of membrane-based oxy-combustion power plants. *Energy*. 2014;70:338–354.
67. Luyben WL. Design and control of distillation columns with intermediate reboilers. *Ind Eng Chem Res*. 2004;43(26):8244–8250.
68. Luyben WL. Design and control of a fully heat-integrated pressure-swing azeotropic distillation system. *Ind Eng Chem Res*. 2008; 47(8):2681–2685.
69. Luyben WL. Design and control of the monoisopropylamine process. *Ind Eng Chem Res*. 2009;48(23):10551–10563.
70. Luyben WL. Design and control of a methanol reactor/column process. *Ind Eng Chem Res*. 2010;49(13):6150–6163.
71. Luyben WL, Chien I-L. *Design and Control of Distillation Systems for Separating Azeotropes*. John Wiley & Sons, Ltd., 2010.
72. Luyben WL. Design and control of the cumene process. *Ind Eng Chem Res*. 2010;49(2):719–734.
73. Luyben WL. Design and control of the methoxy-methyl-heptane process. *Ind Eng Chem Res*. 2010;49(13):6164–6175.
74. Luyben WL. Design and control of a modified vinyl acetate monomer process. *Ind Eng Chem Res*. 2011;50(17):10136–10147.
75. Luyben WL. Design and control of the acetone process via dehydrogenation of 2-propanol. *Ind Eng Chem Res*. 2011;50(3):1206–1218.
76. Luyben WL. Design and control of the butyl acetate process. *Ind Eng Chem Res*. 2011;50(3):1247–1263.
77. Luyben WL. Design and control of the ethyl benzene process. *AIChE J*. 2011;57(3):655–670.
78. Luyben WL. Design and control of the styrene process. *Ind Eng Chem Res*. 2011;50(3):1231–1246.
79. Luyben WL. Design and control of a cooled ammonia reactor. In: Rangaiah GP, Kariwala V, editors. *Plantwide Control: Recent Developments and Applications, Chapter 13*. John Wiley & Sons, Ltd., 2012:273–292.
80. Luyben WL. Design and control of stacked-column distillation systems. *Ind Eng Chem Res*. 2014;53(33):13139–13145.
81. Stefanis SK, Livingston AG, Pistikopoulos EN. Environmental impact considerations in the optimal design and scheduling of batch processes. *Comput Chem Eng*. 1997;21(10):1073–1094.
82. Gebreslassie BH, Yao Y, You F. Design under uncertainty of hydrocarbon biorefinery supply chains: multiobjective stochastic programming models, decomposition algorithm, and a comparison between cvar and downside risk. *AIChE J*. 2012;58(7):2155–2179.
83. Sánchez-Sánchez KB, Ricardez-Sandoval LA. Simultaneous design and control under uncertainty using model predictive control. *Ind Eng Chem Res*. 2013;52(13):4815–4833.
84. Patil BP, Maia E, Ricardez-Sandoval LA. Integration of scheduling, design, and control of multiproduct chemical processes under uncertainty. *AIChE J*. 2015;61(8):2456–2470.
85. Bernardo FP, Pistikopoulos EN, Saraiva PM. Robustness criteria in process design optimization under uncertainty. *Comput Chem Eng*. 1999;23(Suppl. 1):S459–S462.
86. Bernardo FP, Saraiva P, Pistikopoulos EN. Inclusion of information costs in process design optimization under uncertainty. *Comput Chem Eng*. 2000;24(2–7):1695–1701.
87. Bernardo FP, Saraiva PM, Pistikopoulos EN. Process design under uncertainty: robustness criteria and value of information. *Comput Aid Chem Eng*. 2003;16(C):175–208.
88. Bode G, Schomäcker R, Hungerbühler K, McRae GJ. Dealing with risk in development projects for chemical products and processes. *Ind Eng Chem Res*. 2007;46(23):7758–7779.
89. Johnson DB, Bogle IDL. Handling uncertainty in the development and design of chemical processes. *Reliab Comput*. 2006;12(6):409–426.
90. Skogestad S, Morari M. Robust performance of decentralized control systems by independent designs. *Automatica*. 1989;25(1):119–125.
91. Olsen DG, Svrcek WY, Young BR. Plantwide control study of a vinyl acetate monomer process design. *Chem Eng Commun*. 2005; 192(10):12):1243–1257.
92. Arkun Y, Stephanopoulos G. Studies in the synthesis of control structures for chemical processes: part iv. Design of steady-state optimizing control structures for chemical process units. *AIChE J*. 1980;26(6):975–991.
93. Calandranis J, Stephanopoulos G. A structural approach to the design of control systems in heat exchanger networks. *Comput Chem Eng*. 1988;12(7):651–669.
94. Ma K, Valdés-González H, Bogle IDL. Process design in siso systems with input multiplicity using bifurcation analysis and optimisation. *J Process Contr*. 2010;20(3):241–247.
95. Strutzel FAM, Bogle IDL. Assessing plant design with regard to {MPC} performance. *Comput Chem Eng*. 2016;94:180–211.
96. Seferlis P, Georgiadis MC. The integration of process design and control-summary and future directions. *Comput Aid Chem Eng*. 2004;17(C):1–9.
97. Vega P, Lamanna de Rocco R, Revollar S, Francisco M. Integrated design and control of chemical processes—part i: revision and classification. *Comput Chem Eng*. 2014;71:602–617.
98. Ricardez-Sandoval LA, Budman HM, Douglas PL. Integration of design and control for chemical processes: a review of the literature and some recent results. *Ann Rev Contr*. 2009;33(2):158–171.
99. Ricardez-Sandoval LA. Current challenges in the design and control of multiscale systems. *Canad J Chem Eng*. 2011;89(6):1324–1341.
100. Yuan Z, Chen B, Sin G, Gani R. State-of-the-art and progress in the optimization-based simultaneous design and control for chemical processes. *AIChE J*. 2012;58(6):1640–1659.
101. Ghobeity A, Mitsos A. Optimal design and operation of desalination systems: new challenges and recent advances. *Curr Opin Chem Eng*. 2014;6:61–68.
102. Soliman M, Swartz CLE, Baker R. A mixed-integer formulation for back-off under constrained predictive control. *Comput Chem Eng*. 2008;32(10):2409–2419.
103. Francisco M, Vega P, Álvarez H. Robust integrated design of processes with terminal penalty model predictive controllers. *Chem Eng Res Des*. 2011;89(7):1011–1024.
104. Bemporad A, Morari M, Dua V, Pistikopoulos EN. The explicit linear quadratic regulator for constrained systems. *Automatica*. 2002; 38(1):3–20.
105. Kouramas KI, Faísca NP, Panos C, Pistikopoulos EN. Explicit/multi-parametric model predictive control (mpc) of linear discrete-time systems by dynamic and multi-parametric programming. *Automatica*. 2011;47(8):1638–1645.
106. Pistikopoulos EN, Diangelakis NA, Oberdieck R, Papathanasiou MM, Nascu I, Sun M. PAROC—an integrated framework and software platform for the optimisation and advanced model-based control of process systems. *Chem Eng Sci*. 2015;136:115–138.
107. Process Systems Enterprise. gPROMS. www.psenterprise.com/gproms, 1997–2017.
108. Lambert RSC, Rivotti P, Pistikopoulos EN. A monte-carlo based model approximation technique for linear model predictive control of nonlinear systems. *Comput Chem Eng*. 2013;54(0):60–67.
109. Pistikopoulos EN, Faísca NP, Kouramas KI, Panos C. Explicit robust model predictive control. In: *Proceedings of the International Symposium on Advanced Control of Chemical Processes*, ADCHEM'09, 2009:249–254.
110. Kouramas KI, Panos C, Faísca NP, Pistikopoulos EN. An algorithm for robust explicit/multi-parametric model predictive control. *Automatica*. 2013;49(2):381–389.
111. Panos C, Kouramas KI, Georgiadis MC, Pistikopoulos EN. Dynamic optimization and robust explicit model predictive control of hydrogen storage tank. *Comput Chem Eng*. 2010;34(9):1341–1347.
112. Voelker A, Kouramas K, Pistikopoulos EN. Moving horizon estimation: error dynamics and bounding error sets for robust control. *Automatica*. 2013;49(4):943–948.
113. Voelker A, Kouramas K, Pistikopoulos EN. Simultaneous constrained moving horizon state estimation and model predictive control by multi-parametric programming. In: *49th IEEE Conference on Decision and Control*, 2010:5019–5024.
114. Lambert R, Nascu I, Pistikopoulos EN. Simultaneous reduced order multi-parametric moving horizon estimation and model predictive control. In: *Dynamics and Control of Process Systems*, IFAC Proceedings Volumes. Elsevier, 2013:45–50.
115. Pistikopoulos EN. Perspectives in multiparametric programming and explicit model predictive control. *AIChE J*. 2009;55(8):1918–1925.
116. Pistikopoulos EN, Dominguez L, Panos C, Kouramas K, Chinchuluun A. Theoretical and algorithmic advances in multi-parametric programming and control. *Comput Manage Sci*. 2012; 9(2):183–203.
117. Oberdieck R, Diangelakis NA, Papathanasiou MM, Nascu I, Pistikopoulos EN. POP—parametric optimization toolbox. *Ind Eng Chem Res*. 2016;55(33):8979–8991.

118. Oberdieck R, Diangelakis NA, Nascu I, Papathanasiou MM, Sun M, Avraamidou S, Pistikopoulos EN. On multi-parametric programming and its applications in process systems engineering. *Chem Eng Res Des*. 2016;116:61–82.
119. M, Kvasnica B, Takacs J, Holaza SD. Cairano On region-free explicit model predictive control. In: *Proceedings of the IEEE Conference on Decision and Control*, volume 2016-February, 2016: 3669–3674.
120. Bansal V, Sakizlis V, Ross R, Perkins JD, Pistikopoulos EN. New algorithms for mixed-integer dynamic optimization. *Comput Chem Eng*. 2003;27(5):647–668.
121. Chachuat B, Singer AB, Barton PI. Global methods for dynamic optimization and mixed-integer dynamic optimization. *Ind Eng Chem Res*. 2006;45(25):8373–8392.
122. Mitsos A, Chachuat B, Barton PI. Towards global bilevel dynamic optimization. *J Global Optim*. 2009;45(1):63–93. Cited By 12.
123. Flores-Tlacuahuac A, Biegler LT. Simultaneous mixed-integer dynamic optimization for integrated design and control. *Comput Chem Eng*. 2007;31(5–6):588–600. ESCAPE-15 Selected Papers from the 15th European Symposium on Computer Aided Process Engineering held in Barcelona, Spain, May 29-June 1, 2005.
124. Oldenburg J, Marquardt W. Disjunctive modeling for optimal control of hybrid systems. *Comput Chem Eng*. 2008;32(10):2346–2364.
125. Chu Y, You F. Integrated scheduling and dynamic optimization of sequential batch processes with online implementation. *AIChE J*. 2013;59(7):2379–2406.
126. Chu Y, You F. Integration of production scheduling and dynamic optimization for multi-product cstrs: generalized benders decomposition coupled with global mixed-integer fractional programming. *Comput Chem Eng*. 2013;58:315–333.
127. Chu Y, You F. Integrated scheduling and dynamic optimization of complex batch processes with general network structure using a generalized benders decomposition approach. *Ind Eng Chem Res*. 2013;52(23):7867–7885.
128. Chu Y, You F. Integrated planning, scheduling, and dynamic optimization for batch processes: Minlp model formulation and efficient solution methods via surrogate modeling. *Ind Eng Chem Res*. 2014; 53(34):13391–13411.
129. Shi H, Chu Y, You F. Novel optimization model and efficient solution method for integrating dynamic optimization with process operations of continuous manufacturing processes. *Ind Eng Chem Res*. 2015;54(7):2167–2187.
130. Shi H, You F. A novel adaptive surrogate modeling-based algorithm for simultaneous optimization of sequential batch process scheduling and dynamic operations. *AIChE J*. 2015;61(12):4191–4209.
131. Sakizlis V, Perkins JD, Pistikopoulos EN. Parametric controllers in simultaneous process and control design optimization. *Ind Eng Chem Res*. 2003;42(20):4545–4563.
132. Oberdieck R, Diangelakis N, Avraamidou AS, Pistikopoulos EN. On unbounded and binary parameters in multi-parametric programming: applications to mixed-integer bilevel optimization and duality theory. *J Global Optim*. 2016;1–20.
133. Charitopoulos VM, Dua V. Explicit model predictive control of hybrid systems and multiparametric mixed integer polynomial programming. *AIChE J*. 2016;62(9):3441–3460.
134. Diangelakis NA, Avraamidou S, Pistikopoulos EN. Decentralised multi-parametric model predictive control study for domestic chp systems. *Ind Eng Chem Res*. 2016;55(12):3313–3326.
135. Diangelakis NA, Panos C, Pistikopoulos EN. Design optimization of an internal combustion engine powered chp system for residential scale application. *Comput Manag Sci*. 2014;11(3):237–266.
136. Diangelakis NA, Manthanwar AM, Pistikopoulos EN. A framework for design and control optimisation: application on a chp system. In: *Proceedings of the 8th International Conference on Foundations of Computer-Aided Process Design*, *volume 34 of Computer Aided Chemical Engineering*. Elsevier, 2014:765–770.
137. Diangelakis NA, Pistikopoulos EN. A multi-scale energy systems engineering approach to residential combined heat and power systems. *Comput Chem Eng*. 2017;102:128–138.

Manuscript received Dec. 26, 2016, and revision received May 2, 2017.